Analytical and Bioanalytical Chemistry (2018) 410:3991–4014
https://doi.org/10.1007/s00216-018-1013-y

REVIEW

Synthesis and application of magnetic molecularly imprinted polymers in sample preparation

Shuyao Huang[1] · Jianqiao Xu[1] · Jiating Zheng[1] · Fang Zhu[1] · Lijun Xie[2] · Gangfeng Ouyang[1]

Received: 17 November 2017 / Revised: 8 February 2018 / Accepted: 8 March 2018 / Published online: 12 April 2018

Abstract

Magnetic molecularly imprinted polymers (MMIPs) have superior advantages in sample pretreatment because of their high selectivity for target analytes and the fast and easy isolation from samples. To meet the demand of both good magnetic property and good extraction performance, MMIPs with various structures, from traditional core–shell structures to novel composite structures with a larger specific surface area and more accessible binding sites, are fabricated by different preparation technologies. Moreover, as the molecularly imprinted polymer (MIP) layers determine the affinity, selectivity, and saturated adsorption amount of MMIPs, the development and innovation of the MIP layer are attracting attention and are reviewed here. Many studies that used MMIPs as sorbents in dispersive solid-phase extraction of complex samples, including environmental, food, and biofluid samples, are summarized.

Keywords Magnetic molecularly imprinted polymers · Sample preparation · Complex samples · Dispersive solid-phase extraction · Selective extraction

Abbreviations

ATRP	Atom transfer radical polymerization
BPA	Bisphenol A
CNT	Carbon nanotube
DSPE	Dispersive solid-phase extraction
EGDMA	Ethylene glycol dimethacrylate
Fe_3O_4@SiO_2	Silica-coated Fe_3O_4
FRP	Free-radical polymerization
GO	Graphene oxide
HPLC	High-performance liquid chromatography
IF	Imprinting factor
IIP	Ion-imprinted polymer
LCRP	Living/controlled radical polymerization
LOD	Limit of detection
MAA	Methacrylic acid
MIP	Molecularly imprinted polymer
MIT	Molecular imprinting technology
MMIP	Magnetic molecularly imprinted polymer
MNP	Magnetic nanoparticle
MPS	3-(Methacryloxy)propyl trimethoxysilane
RAFT	Reversible addition fragmentation chain transfer
si-ATRP	Surface-initiated atom transfer radical polymerization

Introduction

Magnetic nanomaterials with novel properties have been reported in recent years, and are extensively applied in many fields, such as environmental, food, clinical, and bioanalytical analysis [1]. The feasibility of recovering magnetic nanomaterial by means of an external magnetic field makes it an optimal adsorbent for dispersive solid-phase extraction (DSPE) [2], one of the most commonly used sample preparation methods. Although nanomaterials have a high specific surface area, they also exhibit strong aggregation tendency. To overcome this drawback and endow magnetic nanomaterials with the properties of a satisfactory extraction

✉ Lijun Xie
lijunxie@gdei.edu.cn

✉ Gangfeng Ouyang
cesoygf@mail.sysu.edu.cn

[1] Laboratory of Bioinorganic and Synthetic Chemistry, School of Chemistry, Sun Yat-sen University, Guangzhou, Guangdong 510275, China

[2] Department of Chemistry, Guangdong University of Education, Guangzhou, Guandong 510303, China

amount as well as selectivity, magnetic nanoparticles (MNPs) are modified with various interesting materials, including silica, octadecylsilane, carbon, surfactants, and different types of polymers, which were summarized in a previous review [3]. Unique absorbent coatings result in the MNPs having high adsorption efficiency for target analytes through specific or nonspecific binding, and then after the extraction, the well-dispersed MNPs can be readily isolated from the matrix with use of an external magnetic field without additional filtration or centrifugation. However, with real samples, sorbents face extra challenges; for example, the interfering compounds in the complex matrix may exhibit competitive binding affinities for the sorbent, and finally lead to a decline in performance. So highly selective materials are required for extraction in complex real samples.

Molecularly imprinted polymers (MIPs) with tailor-made binding sites that are complementary to the template molecules in shape, size, and functional groups have attracted extensive attention because of their structure predictability, recognition specificity, and application universality in various fields [4]. Basically, MIPs are obtained by the copolymerization of functional monomers and cross-linkers in the presence of template molecules. After the templates have been eluted, specific tailor-made binding sites are left such that the MIPs are able to recognize the target molecules in terms of the unique size, chemical functionalities, and stereostructure. The combination of MIPs and MNPs gives birth to magnetic MIPs (MMIPs), which have significant advantages in real sample preparation, taking into account the extraction efficiency provided by MNPs and the extraction selectivity provided by MIPs.

Here we review recent applications of MMIPs in sample preparation procedures, emphasizing the preparation of these advanced sorbents and their application in the extraction of some typical analytes in complex samples, including environmental, food, and biological samples.

Fabrication of the MMIP

A typical MMIP is constructed by combination of a magnetic part and an MIP part Several kinds of magnetic materials are used in sample preparation, such as nickel [5], γ-Fe_2O_3 [6–8], Fe_3O_4 [9–12], NiO [13], and their alloys [14]. However, Fe_3O_4 is the most commonly used magnetic material because of its easy fabrication, low toxicity, and most importantly the abundant hydroxyls on the surface, which allow convenient further modification [3]. Fe_3O_4 nanoparticles can be easily synthesized by coprecipitation [15–17]. A solvothermal method is another common choice for Fe_3O_4 preparation [18–21]. For better dispersion, Fe_3O_4 nanoparticles are usually coated with oleic acid before further modification [11]. Silica-coated Fe_3O_4 (Fe_3O_4@SiO_2) is also a common choice because the SiO_2 layer is a good medium for immobilizing different functional groups on the surface of the MNPs [12].

During the sample preparation procedure, a higher extraction amount, selectivity, and efficiency are persistently demanded. The composition of MIPs determines the selectivity and affinity for target analytes, so molecular imprinting technologies (MITs) should be carefully chosen or designed before being applied. Since the number of accessible binding sites and the specific surface area of MMIPs have a great influence on the maximum extraction amounts, MMIP composites with different structures have also been reported.

Molecular imprinting strategies

The MIP layer endows the sorbent material with selective recognition capacity toward target analytes, so the design of the MIP layer is of great importance during MMIP fabrication. MITs have continuously been developed since the discovery of molecular imprinting, especially in the last 20 years [4]. A number of smart MIT strategies based on the two traditional polymerization principles—free-radical polymerization (FRP) [22] and sol–gel polymerization [23]—have been proposed [4]. To realize successful molecular imprinting, MIT should be applied to from strong and specific binding between templates and functional monomers. To obtain a good-performing MIP layer with more accessible binding sites, various magnetic composites with high specific surface area were developed and served as the supporters for imprinting.

Free-radical polymerization

FRP is one of the most popular and well-developed synthesis methods used in preparing MIPs. FRP can be realized in indifferent ways, including suspension polymerization [24], emulsion polymerization [25], and precipitation polymerization [26], for which the differences and advantages were summarized in detail in a previous review [4]. To fabricate a desired MMIP, active groups (such as a carbon–carbon double bond) will be firstly grafted on the MNPs for better surface immobilization. Then after the initiators have been added, the FRP starts among the surface-grafted active groups, the monomers, and the cross-linkers under vigorous stirring and N_2 protection (Fig. 1a).

Organic acrylate or acrylic-based MIPs are mainly prepared by radical polymerization [4]. Different functional monomers are designed to form specific donor–receptor or antibody–antigen complexes with the templates, from organic molecules [29] to inorganic ones [30]. The variety of functional monomers endows FRP with general applicability. Among them, methacrylic acid (MAA) is the most commonly used monomer according to Zhang et al. [31], who revealed in detail the versatility of MAA in FRP.

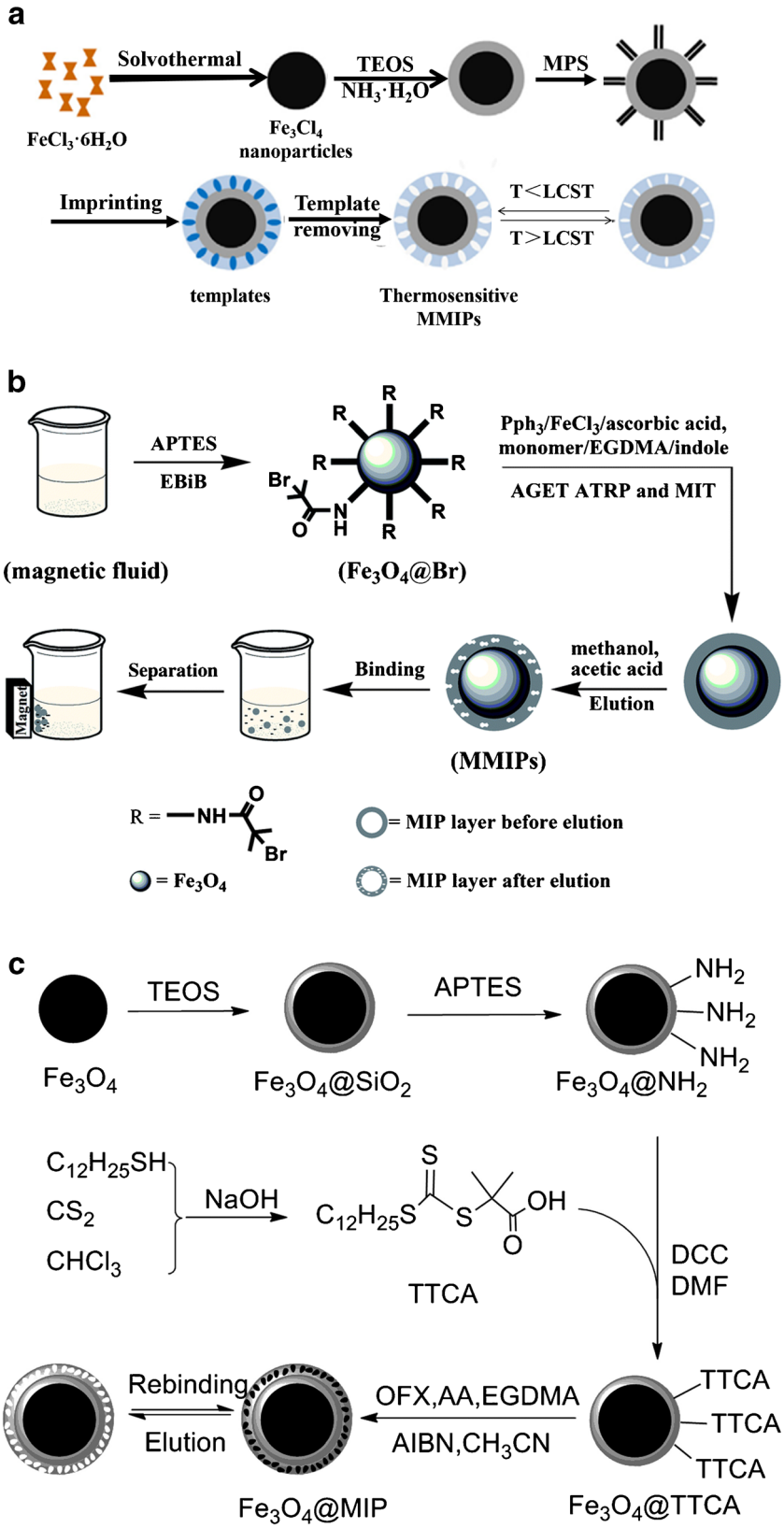

Fig. 1 Preparation of core–shell magnetic molecularly imprinted polymers (MMIPs) through **a** typical free-radical polymerization, **b** activator generated by electron transfer atom transfer radical polymerization (AGET ATRP), and **c** reversible addition fragmentation chain transfer polymerization. AA acrylic acid, AIBN 2,2-azobisisobutyronitrile, APTES 3-aminopropyltriethoxysilane, DCC *N*,*N*′-dicyclohexylcarbodiimide, DMF dimethyl formamide, EBiB 2-bromoisobutyryl, EGDMA ethylene glycol dimethacrylate, LCST lower critical solution temperature, MIT molecular imprinting technology, MIP molecularly imprinted polymer, MPS 3-(methacryloxy)propyl trimethoxysilane, OFX ofloxacin, TEOS tetraethoxysilane, TTCA *s*-1-dodecyl-*s*′-(α,α′-dimethyl-α"-aceticacid. (**a** From [21], copyright 2014 Elsevier; **b** from [27], copyright 2014 Royal Society of Chemistry; **c** from [28], copyright 2014 American Chemical Society)

FRP has been continuously used and developed for decades because of its simple production and wide application. However, particles with irregular sizes are always obtained because of the uncontrollable chain propagation rate and side reactions (including chain transfer and termination) [4, 32]. The binding of analytes to and their dissociation from the inner binding sites

will be more difficult because the transfer distances are extended, which might lead to a decline of extraction efficiency.

Living/controlled radical polymerization

The living/controlled radical polymerization (LCRP) technique is a newly developed method in which dormant species (such as alkyl halides) are introduced into the system to maintain the concentration of active radicals at a low level [33]. The negligible chain termination and a more constant reaction rate result in a controllable polymerization procedure. In this way a thin and uniform MIP layer can be obtained.

Atom transfer radical polymerization (ATRP) is one of the most promising methods among LCRP strategies. By using transition metal complexes as the reversible halogen atom transfer reagents, ATRP can establish a fast, dynamic equilibrium between the dormant species (alkyl halides) and active radicals [33]. As reported by Liu et al. [34], a bromide-grafted MNP (Fe_3O_4@SiO_2@Br) was used as the initiator, and a typical transition metal compound (CuBr) served as the catalyst under N_2 protection. As a result, a uniform thin MIP layer was fabricated, the thickness of which was only 18 nm. However, there is a limitation that strictly anaerobic conditions are required because of the easy oxidization of the transition metal initiator, which might impose great restrictions on the reaction [27]. Many efforts have been devoted to solve this problem [35]. For instance, Liu et al. [27] developed a method based on activator generated by electron transfer ATRP to prepare indole-imprinted MMIPs (Fig. 1b). By addition of reducing agents (iron chloride hexahydrate, PPh_3, and ascorbic acid) to the reaction solution, the polymerization can be conducted in ambient conditions.

Reversible addition fragmentation chain transfer (RAFT) is another attractive method to prepare MIPs, because of its relatively mild reaction conditions [4]. Chain transfer agents (azo initiators, iniferters, RAFT agents, etc.) [28, 36–39] were synthesized and introduced on the surface of the magnetic supports, which subsequently dispersed in the solution and participated in the following polymerization (Fig. 1c).

By use of these novel LCRP strategies, uniform imprinted layers with adjustable thickness (usually at the nanometer level) can be obtained, which ensures the accessibility of binding sites of MMIPs and fast mass transfer during the extraction [28]. As the high specific surface area of nanoparticles is made full use of, the extraction capacity of MMIPs is increased as well. However, the number of suitable initiators or transfer agents is still limited [4] and the LCRP procedures are complex in comparison with those of traditional FRP, which hinder the wider application of LCRP.

Sol–gel polymerization

During the FRP procedure, a highly toxic solvent such as chloroform, acetonitrile, or toluene is used in large quantities. An alternative polymerization method, sol–gel polymerization, attracted great interest because of the use of some eco-friendly reaction solutions (such as water or ethanol) and more importantly, its mild fabrication procedure [4]. In the sol–gel process, precursors such as tetramethoxysilane [40], tetraethoxysilane [41], or other tetraalkoxysilanes [42], are firstly hydrolyzed (forming a sol) and then gradually polymerized (or condensed) to form cross-linked silica materials (or gels) [23]. The silica polymers obtained are rigid and have a high degree of cross-linking, because of the short distance between the cross-link sites. As a result, the sol–gel silica exhibits not only good chemical stability in most conditions but also minimal swelling behavior in the presence of a solvent compared with the polymers synthesized by FRP [43]. This allows silica MIPs to maintain the shape or size of the binding sites, which results in better recognition of target analytes. Besides, the fabrication conditions of sol–gel polymerization are mild [23], which is required during the imprinting of some molecules, enzymes, or antibodies, for example, without damaging their activities [28].

Self-polymerization of dopamine

Besides the aforementioned MITs, the self-polymerization of dopamine has attracted extensive attention in MIP fabrication recently [44, 45], because its preparation is extremely simple, and the polydopamine obtained exhibits not only excellent mechanical strength but also abundant binding sites (catechol and amine groups). Li et al. [46] developed a protein-imprinting magnetic microsphere on a SiO_2-coated Fe_3O_4 nanoparticle. After the MIP layer had been obtained, the polydopamine was subsequently modified to form phospholipid brushes to avoid nonspecific adsorption on the surface, which ensures the selectivity of the MMIP particles for the target protein. Another advantage of this strategy is that the thickness of the polydopamine layer can be controlled by adjustment of the polymerization conditions or the reaction time [47], which shows great potential for successful surface imprinting.

Structures of MMIPs

To meet the requirements for analysis of different target analytes in different samples, various structures of MMIPs have been reported. A core–shell structure, of which the magnetic phase is the core and the polymeric phase acts as the shell, is the most widely used one [48]. The polymer coating prevents the core from being oxidized and aggregating, but at the same time weakens the magnetic performance. To ensure the ratio of magnetic part in MMIPs, multicore MMIPs [49] were synthesized, and satisfactory results were obtained. However, the magnetic core, with no recognition ability, possesses most of the mass of the MMIP, which greatly decreases

the binding capacity, so various assembled MMIPs [50–52] with a larger accessible surface area were developed. In this section, the fabrication of MMIPs with typical structures (Fig. 2) is briefly summarized.

Core–shell MMIPs

Since the first MMIP bead was prepared by Ansell and Mosbach [59] in 1998, the core–shell structure has been widely used because this structure fully utilizes the high specific surface area of MNPs and it is easy to fabricate. Although active hydroxyl groups are on the surface of the Fe_3O_4 particle, Fe_3O_4@SiO_2 is more commonly used because the SiO_2 layer protects the core from oxidation or dissolution in the following reactions [3]. Fe_3O_4@SiO_2 is considered a suitable supporter for both sol–gel polymerization and FRP. The MIP layer can be conveniently grown on the surface without further modification in sol–gel polymerization [60], whereas for FRP, modification is also easy to achieve as vinyl groups can be introduced through the reaction between the surface Si–OH groups and molecules such as 3-(methacryloxy)propyl trimethoxysilane (MPS) [29]. Recently, another protector polymer was used by Liu et al. [61]; a polychloromethylstyrene layer was compactly grown on the surface of Fe_3O_4 nanoparticles. After alkali treatment, hydroxyl-rich particles (Fe_3O_4@polystyrene@OH) were obtained. Then 2-bromoisobutyryl was immobilized, and the particles were used as macroinitiators for further imprinting by surface-initiated ATRP (si-ATRP). Finally, a well-controlled MMIP was obtained and showed excellent selective and highly efficient extraction of bisphenol A (BPA).

Magnetic-nanotube-supported MIPs

Typically, acidified nanotubes are added to the mixture during the coprecipitation or solvothermal reaction of Fe_3O_4 so that magnetic particles can be easily attached on the nanotubes (Fig. 2b). Ma et al. [52] coated the surface of magnetic carbon nanotubes (CNTs) with SiO_2 and then used them as the supporter for a typical FRP. By the formation of a composite with CNTs, the synthesized MMIP exhibited a higher specific surface area, and was applied for trace analysis of pyrethroids in fruit matrices. Another example was reported by Xiao et al. [62]. Here, magnetic CNTs coated with MIPs were prepared for extraction of levofloxacin in serum samples. Compared with the traditional core–shell MMIPs, although the adsorption kinetics were similar, the assembled MMIPs possessed greater adsorption capacity, probably because the higher specific surface area led to more binding sites. Similar work was reported by the same group for the determination of gatifloxacin in serum samples [63].

Besides a larger specific surface area, these novel structures also provide us with new strategies to fabricate water-compatible MMIP materials. The extraordinarily high aspect ratio of nanotubes also makes them good substrates for oriented immobilization [64]. Inspired by a biomimetic *Setaria viridis*-like structure, Ma et al. [64] provided a general approach for preparing a hydrophilic magnetic core–shell nanotube by surface molecular imprinting. Firstly, Fe_3O_4 nanoparticles were anchored on halloysite nanotubes ($Al_2Si_2O_5(OH)_4 \cdot nH_2O$), on which further modification and initiator grafting were performed. Subsequently, si-ATRP was performed for the molecular imprinting, and then a hydrophilic layer—poly(2-hydroxyethyl methacrylate)—was grafted on the outer surface by another ATRP. MMIPs with a similar brush structure were also synthesized by Dai et al. [56]; the fabrication procedure is shown in Fig. 2c.

Magnetic-nanosheet-supported MIPs

Graphene possesses not only a high specific surface area but also a large conjugation system, which endows it with strong affinity for carbon-based ring molecules. This characteristic allows large amounts of templates to be enriched on the graphene surface before the MIP procedure, so abundant recognition sites will be left after template elution. An MIP-coated magnetic graphene composite was fabricated by Luo et al. [51] to extract 4-nitrophenol. The polymerization conditions were optimized to obtain an MIP layer with a suitable thickness (16–30 nm). A satisfactory result was obtained in that the composite exhibited high adsorption capacity (142 mg g^{-1}) as well as an extremely fast adsorption rate (2 min to extraction equilibrium). Magnetic particles were also immobilized on graphene oxide (GO) to act as the support for molecular imprinting, which was reported by Ning et al. [65].

Porous-material-supported MMIPs

Besides the aforementioned structures, some interesting structures were also reported (Fig. 2). For example, a well-designed magnetic hollow porous MIP (Fig. 2d) was prepared for specific enrichment of trace protocatechuic acid by Li et al. [50]. In this work, a mesoporous material, MCM-48 (a kind of mesoporous molecular sieve), was used as a sacrificial support, on which molecular imprinting occurred. After the template and silica had been removed, the epoxide ring of glycidyl methacrylate was opened, and finally Fe_3O_4 was attached by coprecipitation. The hollow structure provided highly dense accessible recognition sites for molecular imprinting, such that the equilibrium adsorption amount was 37.7 mg g^{-1} in 25 min, which was a significant increase in capacity as well as efficiency compared with traditional MIPs.

MMIP sorbents with a nanoring structure can be obtained by suspension polymerization (Fig. 2e) [53, 66]. Zhao et al [66] firstly constructed a magnetic nanoring with abundant epoxy groups on the surface, and then imprinted BPA by the ring-opening reaction between epoxy and polyamine. The synthesized MMIP exhibited about three times greater

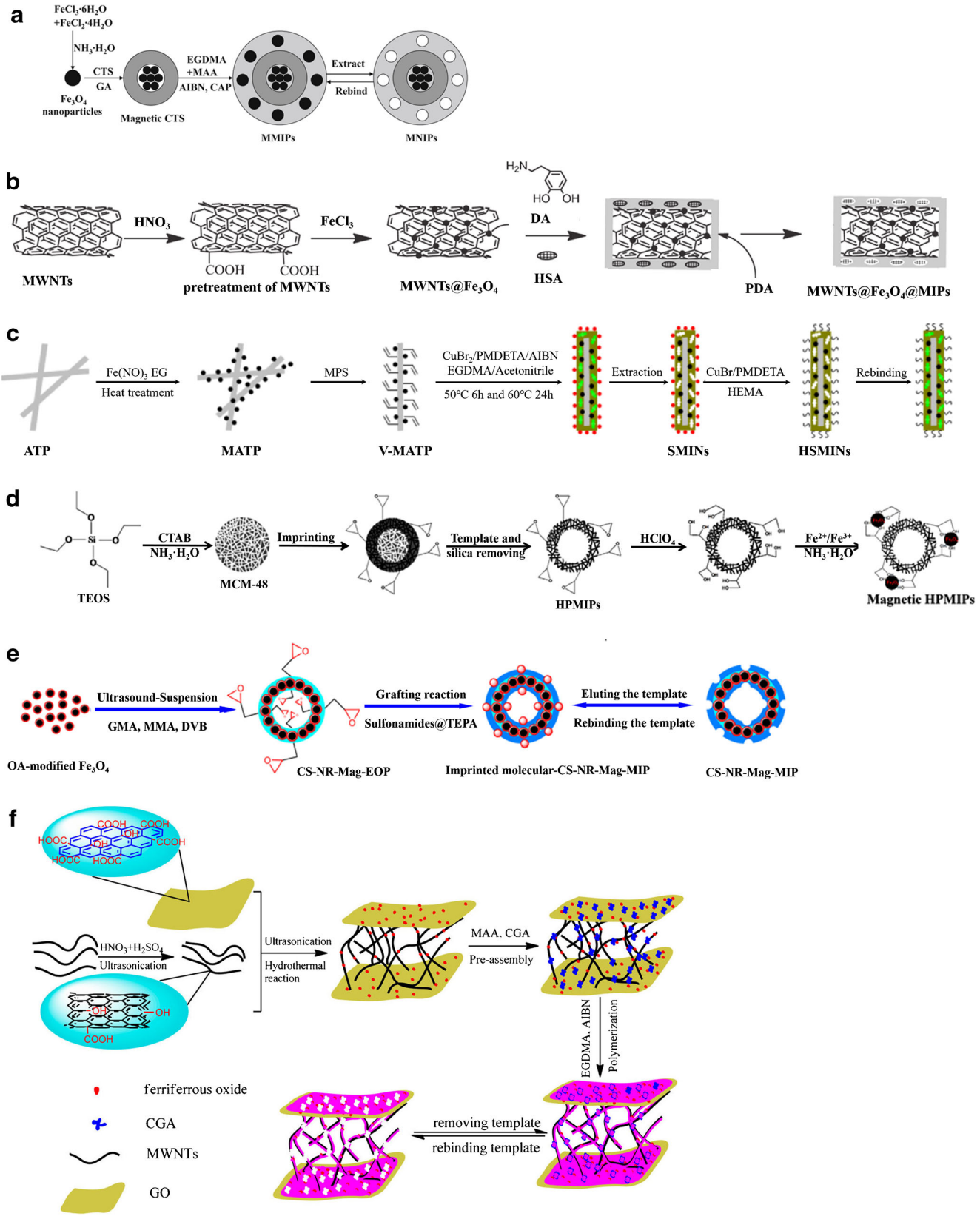
a
$FeCl_3{\cdot}6H_2O$ +$FeCl_2{\cdot}4H_2O$
$NH_3{\cdot}H_2O$
CTS
GA
Fe_3O_4 nanoparticles
Magnetic CTS
EGDMA +MAA AIBN, CAP
MMIPs
Extract
Rebind
MNIPs
b
MWNTs
HNO_3
COOH COOH
pretreatment of MWNTs
$FeCl_3$
MWNTs@Fe_3O_4
DA
HSA
PDA
MWNTs@Fe_3O_4@MIPs
c
ATP
$Fe(NO_3)$ EG
Heat treatment
MATP
MPS
V-MATP
$CuBr_2$/PMDETA/AIBN
EGDMA/Acetonitrile
50°C 6h and 60°C 24h
Extraction
SMINs
CuBr/PMDETA
HEMA
HSMINs
Rebinding
d
TEOS
CTAB
$NH_3{\cdot}H_2O$
MCM-48
Imprinting
Template and silica removing
HPMIPs
$HClO_4$
Fe^{2+}/Fe^{3+}
$NH_3{\cdot}H_2O$
Magnetic HPMIPs
e
OA-modified Fe_3O_4
Ultrasound-Suspension
GMA, MMA, DVB
CS-NR-Mag-EOP
Grafting reaction
Sulfonamides@TEPA
Imprinted molecular-CS-NR-Mag-MIP
Eluting the template
Rebinding the template
CS-NR-Mag-MIP
f
HNO_3+H_2SO_4
Ultrasonication
Ultrasonication
Hydrothermal reaction
MAA, CGA
Pre-assembly
EGDMA, AIBN
Polymerization
removing template
rebinding template
ferriferrous oxide
CGA
MWNTs
GO

◀ **Fig. 2** The fabrication protocols for assembled magnetic molecularly imprinted polymers (MMIPs). **a** The synthesis of chloramphenicol (CAP)-imprinted MMIPs with multimagnetic cores and a chitosan (CTS) complex as the supporter. **b** The preparation of MMIPs on Fe_3O_4-immobilized multiwalled nanotubes (MWNTs) via dopamine (DA) self-assembly. **c** The synthesis procedure for surface imprinting of magnetic attapulgite (MATP) with ultrathin hydrophilic polymer brushes. **d** The synthesis procedure for preparing magnetic hollow porous molecularly imprinted polymers (MIPs). **e** The procedure for preparing core–shell nanoring MMIPs [53]. **f** The synthesis of 3D MMIPs based on a magnetic graphene–carbon nanotube composite. AIBN 2,2-azobisisobutyronitrile, ATP attapulgite, CGA chlorogenic acid, CTAB cetyltrimethyl ammonium bromide, DVB divinylbenzene, EG ethylene glycol, EGDMA ethylene glycol dimethacrylate, GA glutaraldehyde, GMA glycidyl methacrylate, GO graphene oxide, HEMA 2-hydroxyethyl methacrylate, HPMIP hollow porous molecularly imprinted polymer, HSA human serum albumin, MAA methacrylic acid, MMA methyl methacrylate, MPS 3-(methacryloxy)propyl trimethoxysilane, CS-NR-Mag-EOP core-shell nanoring magnetic epoxy polymer , CS-NR-Mag-MIP core shell nanoring magnetic molecularly imprinted polymer, OA oleic acid, PDA polydopamine, PMDETA *N*,*N*,*N*′,*N*′,*N*″-pentamethyl diethyenetriamine, SMIN surface imprinted nanocomposite, TEOS tetraethoxysilane, TEPA tetraethyleneprntamine, V-MATP vinyl-modified magentic attapulgite . (**a** From [54], copyright 2014 Springer; **b** from [55], copyright 2015 Elsevier; **c** from [56], copyright 2014 Wiley Periodicals; **d** from [50], copyright 2015 Elsevier; e from [53]; **f** from [57], copyright 2016 American Chemical Society)

extraction capability than traditional nanosphere MMIPs and showed good selectivity. A material with a similar structure [53] was also fabricated (Fig. 2e) and applied in the sensitive determination of 22 sulfonamides. Even in complex samples, such as chicken breast muscle, the limit of detection (LOD) of the method was 0.004–0.030 ng g^{-1}.

Compared with the aforementioned MMIP structures, compositing various porous materials with a magnetic MIP showed an extra advantage; that is, the easier mass transfer between the MIP layer and the sample matrices, which is mainly due to the highly porous structures. It was suggested that the binding sites would not be fully accessible as the diffusion paths are much more tortuous in the high-density polymers and air might be trapped [58], which would lead to a decline of the extraction efficiency. However, the fabrication required multistep reactions, so development of a concise protocol for construction of this kind of MMIP is demanding.

Application of MMIPs

Serving as DSPE sorbents is the most recognized application of MMIPs in the analytical field. After the extraction or elution, MMIP particles can be easily collected by use of an external magnetic field rather than centrifugation or filtration [67]. So using MMIPs could efficiently simplify the procedure and reduce the preparation time by virtue of the introduced magnetic materials [68]. However, the successful purification (selective extraction) and the efficient enrichment are key factors for good analytical performances, especially in the detection of trace- or ultratrace-level analytes in complex sample matrices, such as environmental, food, and biological samples. To address these points, great effort has been made in designing suitable MMIPs with higher affinities for different target analytes.

The interaction between the imprinting sites and the target analytes can be divided into three types [4]: covalent interactions (reversible bonding), noncovalent interactions (hydrogen bonding, electrostatic interaction, coordination bonding, etc.), and semicovalent interactions (the template is bound covalently to the functional monomer but the extraction is based on noncovalent interactions) [69, 70]. Depending on the different analytes, choosing a suitable interaction mechanism also plays an important role in improving the analytical performance.

MMIPs in environmental samples

Pesticides or herbicides

Pesticides (or insecticides) and herbicides are widely used in agriculture to reduce the harm caused by some insects and weeds, and their use has greatly increased crop quality and quantity. These substances are mainly organic compounds with characteristic functional groups, which would be considered ideal interaction sites for molecularly imprinting.

For example, triazine herbicides, which contain a triazine ring and identical secondary amino groups, are widely used in cereal plants. Multiple hydrogen bonds [29] can be formed between the nitrogen atoms in the target molecules and the outer carboxyl groups. The FRP technique was widely applied because the typical functional monomers for FRP, such as MAA [71, 72], can form effective imprinting sites. Men et al. [29] synthesized a core–shell MMIP material for selective extraction of atrazine in corn and river water. After vinyl groups had been grafted on the silica-coated MNPs (Fe_3O_4@SiO_2-MPS), the MIP layer was fabricated with MAA as the functional monomer, ethylene glycol dimethacrylate (EGDMA) as the cross-linker, atrazine as the template, and 2,2-azobisisobutyronitrile as the initiator. The recognition capacity of the synthesized MMIP was evaluated, and the equilibrium extraction amount was 1.775 μmol g^{-1}. However, with this material, 5 h was needed to reach equilibrium. Qiao et al. [71] reported an alternative way for preparing MMIP targeting two triazines, cyanazine and atrazine, by water/oil/water suspension polymerization. In this work, water-compatible particles with a narrow size distribution (10–18 nm) were ultimately obtained. By the coupling of off-line DSPE with high-performance liquid chromatography (HPLC)–UV analysis, the LODs of this method (cyanazine 0.25 ng mL^{-1} atrazine, 0.37 ng mL^{-1}) were ten times lower than the LOD of the method developed by Men et al. Moreover, the extraction equilibrium was reached in only 5 min.

Organophosphate pesticides [73], sulfonylurea herbicides [74], and pyrethroid pesticides [52, 75, 76] are also extensively used in agriculture (see Table 1). In the molecules, nitrogen

Table 1 Application of magnetic molecularly imprinted polymers in sample preparation procedures for pesticide analysis

Polymerization method	Magnetic materials	Monomer; cross-linker; initiator; template	Sample	Analyte	Analytical techniques	LODs (ng mL^{-1})
Suspension polymerization	Fe_3O_4	MAA; TRIM; AIBN; cyromazine	Environmental water	Cyanazine, ATZ	HPLC–UV detection	0.25, 0.37
Microwave irradiation FRP	Fe_3O_4/PEG	MAA; TRIM, DVB; AIBN; ATZ	Tomato, strawberry juice, milk	Triazines	HPLC	0.20–0.63
Suspension polymerization	Fe_3O_4/PEG	MAA; TRIM; AIBN; ATZ	Soil, food samples	7 triazines	HPLC–UV detection	2.10-8.17
RFP	Fe_3O_4@SiO_2-MPS	MAA; EGDMA; AIBN; ATZ	Corn, river water	ATZ	HPLC–UV detection	5, 3
FRP	Fe_3O_4@PEG	MAA, HEMA; EGDMA; AIBN; diazinon	Soil, cucumber	Diazinon	HPLC	5
FRP	Fe_3O_4@SiO_2	MAA; EGDMA; AIBN; diazinon	Food samples, water samples	Diazinon	HPLC–UV detection	0.02
FRP	Fe_3O_4@SiO_2-MPS	MAA; TRIM; $K_2S_2O_8$; CPF	Rice	CPF	HPLC–UV detection	0.0072 μg·g^{-1}
FRP	Fe_3O_4@SiO_2-MPS	MAA; EGDMA; AIBN; methyl parathion	Soil	Methyl parathion	HPLC	5.2 ng·g^{-1}
Sol–gel polymerization	MCNT@SiO_2	APTES; TEOS; nicosulfuron	Grains	Sulfonylureas	HPLC–UV detection	0.0107-0.0151
FRP	Fe_3O_4@SiO_2-MPS	MAA; TRIM; AIBN; bensulfuron-methyl	Water, soil, grain	4 sulfonylureas	HPLC–UV detection	6.4-9.5 nmol·mL^{-1}
FRP	Fe_3O_4@SiO_2-MPS	MAA; TRIM; AIBN; metsulfuron-methyl	Environmental water samples	5 sulfonylureas	LC–DAD	0.02-0.03
FRP	Fe_3O_4@SiO_2-MPS	AM, allyl fluorescein; DVB; AIBN; LC	Honey	λ-Cyhalothrin	fluorescence spectrophotometer	2.3
FRP	Fe_3O_4/CD	MMA; MBAA; $K_2S_2O_8$; template–β-CD	Vegetable samples	Dicofol, pyridaben	GC–MS	1.0, 3.2 pg·g^{-1}
FRP	Fe_3O_4@Au-β-CD	MAA; MBAA; ultrasonic; carbendazim	Vegetables	Carbendazim	HPLC–UV–vis detection	0.0030
Sol–gel polymerization	MCNT@SiO_2	APTES; HAc; propoxur	Fruits	Carbamates	HPLC–UV detection	9.7-12 ng·g^{-1}
FRP	Fe_3O_4@OA	MAA; EGDMA; AIBN; DDT	Tea	Dicofol	GC–ECD	0.05
Suspension polymerization	Fe_3O_4@OA	IL, MAA; EGDMA; AIBN;4,4′-dichlorobenzhydrol	Environmental water samples	Organochlorine pesticides	GC–ECD	0.12-0.26
FRP	MCNT@SiO_2-MPS	MAA; EGDMA; cyhalothrin	Fruit samples	β-Cyfluthrin, cyhalothrin, cyphenothrin,permethrin	HPLC–UV detection	7.2, 3.5, 6.2, 6.8

Polymerization method	Linear range (ng mL^{-1})	Recovery (%)	Saturation magnetization (emu g^{-1})	Recognition capacity (mg g^{-1})	Recognition kinetics (min)	Reference
Suspension polymerization	2.5-200.0	84.8-104.3	-	36.0, 38.0	5	[71]
Microwave irradiation FRP	1.0–40.0	71.6-118.5, 80.3-112.9, 82.1-113.2	-	-	240	[77]
Suspension polymerization	5.00-50.00	71.6-126.7	0.491	86-137 pmol	30	[72]
RFP	100-2000, 100-1500	94.0-98.7, 88.7-93.5	1.15	1.775 μmol g^{-1}	300	[29]
FRP	20-5000	85, 88	-	-	-	[78]
FRP	0.07-30.0	96.0-104.0	-	24.6	20	[79]
FRP	0.025-10 μg·g^{-1}	81.2-92.1	10.15	92.71	10	[80]
FRP	15-2500	81.1-87.0	24.38	9.1	5	[81]

Table 1 (continued)

Polymerization method	Linear range (ng mL^{-1})	Recovery (%)	Saturation magnetization (emu g^{-1})	Recognition capacity (mg g^{-1})	Recognition kinetics (min)	Reference
Sol–gel polymerization	0.05-10	82.2-98.0	23.68	32.11	20	[82]
FRP	0.04-0.8 nmol·mL^{-1}	78.1-102.0, 80.8-95.8, 93.2-91.5	13.4	37.32	180	[74]
FRP	0.10-10	94.3-102.3	-	-	-	[83]
FRP	0-50 nmol L^{-1}	98-107	8.84	-	-	[84]
FRP	1-2000	92.8-105.2, 94.4-104.6	-	260, 220	30, 25	[85]
FRP	2-1000	90.5-109	52.0	190	30	[86]
Sol–gel polymerization	40-10,000	90.5-98.6	17.66	17.1	30	[87]
FRP	0.2-160	83.6-94.5	56.8	-	5	[88]
Suspension polymerization	1.0-100	82.6-100.4	-	0.119 mmol g^{-1}	-	[89]
FRP	25-5000	84.2-101.7	8.64	255.04	-	[52]

AIBN 2,2-azobisisobutyronitrile, *AM* acrylamide, *ATZ* atrazine, *CD* cyclodextrin, *CPF* chlorpyrifos, *DDT* dichlorodiphenyltrichloroethane, *DVB* divinylbenzene, *ECD* electron capture detection, *EGDMA* ethylene glycol dimethacrylate, *FRP* free-radical polymerization, *GC* gas chromatography, *HEMA* 2-hydroxyethyl methacrylate, *HPLC* high-performance liquid chromatography, *IL* ionic liquid, *LC* liquid chromatography, *LC–DAD* liquid chromatography–diode array detection, *LOD* limit of detection, *MAA* methacrylic acid, *MBAA N,N'*-methylenebisacrylamide, *MCNT* magnetic carbon nanotube, MPS 3-(methacryloxy)propyl trimethoxysilane, *MS* mass spectrometry, *OA* oleic acid, *PEG* polyethylene glycol, *RFP* free radical polymerization, *TRIM* trimethylolpropane trimethacrylate

and oxygen atoms serve as recognition sites via hydrogen bonds in molecular imprinting. However, functional groups containing these atoms might inhibit or retard the FRP [90], or even lead to the failure of imprinting. To overcome this drawback, Masoumi et al. [90] used a synthesized copolymer, poly(methyl methacrylate-*co*-maleic anhydride), as the monomer, and the MIP layer was immobilized on the surface of Fe_3O_4–NH_2 nanoparticles via an amidation reaction. The materials obtained exhibited much higher maximum adsorption capacities (more than 192.3 mg g^{-1}) than the material obtained by the traditional FRP method (24.6 mg g^{-1}) [79]. But the use of polymer monomer led to a compact structure of the MIP layer, which had a negative influence on mass transfer, as the equilibrium extraction took more than 60 min.

Antibiotics

Antibiotics are a class of pharmaceuticals used as chemotherapeutic agents for the prevention and treatment of human and animal diseases, and as growth promoters in livestock farming or agriculture. However, some of the antibiotic is not assimilated, and is excreted into the environment [91], which causes wide public concern. Antibiotics can be divided into various types (including quinolones [28], sulfonamides [92–94], tetracyclines [95, 96], macrolides [96–98], amphenicols [99], and β-lactams [100]) according to their characteristic molecular structures. Similarly to the aforementioned pesticides, noncovalent binding via hydrogen bonds is the major interaction strategy for antibiotic imprinting [28, 93, 101, 102]. However, during the real sample extraction (mainly in aqueous systems), water molecules will interfere with the rebinding between target analytes and the MIP, so stronger interactions are always desired. Qin et al. [92] synthesized a novel core–shell MMIP, using sulfamethazine and sulfamethoxazole as the mixing templates, in which *p*-aminobenzamide was the fundamental structure. Serving as the functional monomer, 2-vinylpyridine can not only form hydrogen bonds with the sulfate or amino groups but can also undergo π–π interaction with the aromatic rings. By the coupling with HPLC–UV detection, the method exhibited extremely low LODs (5.46–12.13 ng L^{-1}) and wide linear ranges (10.0–2000.0 ng L^{-1}) for seven structurally similar sulfonamides compared with other studies (see in Table 2).

In other work [104], MMIPs targeting fluoroquinolones were synthesized with use of a magnetic CNT composite as the supporter, glycidyl methacrylate as the functional monomer, and divinylbenzene as the cross-linker. On one hand, the supporter CNT endowed the fluoroquinolones with a good enrichment property through the conjugation and its high specific surface area. On the other hand, the cross-linker divinylbenzene could also interact with the heterocyclic rings. As a result, MIPs with highly specific binding sites were obtained. Compared with previous work [101, 102], the method

Table 2 Application of magnetic molecularly imprinted polymers in sample preparation procedures for antibiotic analysis

Polymerization method	Magnetic materials	Monomer; cross-linker; initiator; template	Sample	Analyte	Analytical techniques	LODs (ng mL^{-1})
FRP	Fe_3O_4@OA	MAA; EGDMA; AIBN; SMD	Water	Sulfonamides and their metabolites	LC–MS/MS	0.38-1.32 ng L^{-1}
FRP	Fe_3O_4-CS	2-VP; TRIM; AIBN; SMZ, SMX	Wastewater	Sulfonamides	HPLC–UV detection	5.46-12.13 ng L^{-1}
AGET ATRP	γ-Fe_2O_3@SiO_2-MPS	MAA; EGDMA; ZnO@SiO_2-Br; SMZ	Pork	Sulfamethazine	HPLC–UV detection	19.0 μg L^{-1}
FRP	Fe_3O_4@OA	MAA; EGDMA; AIBN; ciprofloxacin	Water samples	Fluoroquinolone	LC–MS/MS	3.2-6.2 ng L^{-1}
FRP	Fe_3O_4@POSS	MAA; POSS; AIBN; enrofloxacin	Milk	Fluoroquinolones	HPLC–UV detection	1.76-12.42
RAFT	Fe_3O_4@SiO_2@TTCA	AA; EGDMA; AIBN; OFX	Human urine	Fluoroquinolones	HPLC	8.5-19.4
FRP	Fe_3O_4@CCNs	MAA; DVB; AIBN; ciprofloxacin	Egg	Fluoroquinolones	HPLC	3.6-18.4 ng g^{-1}
FRP	EDA@MCNTs	GMA; DVB; AIBN; danofloxacin	River water	Fluoroquinolones	UFLC–MS/MS	0.088-0.59 ng L^{-1}
FRP	Fe_3O_4@m-SiO_2-V	VTMOS; EGDMA; $K_2S_2O_8$; CAP, FF	Water, blood, egg	Amphenicol	HPLC–UV detection	0.08-0.16 ng g^{-1}
FRP	Fe_3O_4	MAA; TRIM; AIBN; OTC, TCT	Egg, honey	Tetracyclines	HPLC–UV-DAD	1.0-125 ng g^{-1}
FRP	Fe_3O_4@OA	MAA; DVB; AIBN; OTC	Egg and tissue	Tetracycline	LC–MS/MS	0.2 ng g^{-1}
FRP	Fe_3O_4@OA	MAA; EGDMA; AIBN; PENV	Milk	β-Lactam	LC–MS/MS	1.6-2.8
FRP	Fe_3O_4@SiO_2-MPS	MAA; EGDMA; AIBN; ERY	Pork, fish, shrimp	macrolide	HPLC–UV detection	0.015-0.2 μg g^{-1}
FRP	Fe_3O_4@SiO_2	MAA; EGDMA; AIBN; roxithromycin	Human plasma	Roxithromycin	LC–MS/MS	3.8-9.8
FRP	MMWCNTs@PMMA	MAA; EGDMA; AIBN; erythromycin	Fish	Erythromycin	HPLC	9.7

Polymerization method	Linear range (ng mL^{-1})	Recovery (%)	Saturation magnetization (emu g^{-1})	Recognition capacity (μmol g^{-1})	Recognition kinetics (min)	Reference
FRP	5-500 ng L^{-1}	30.8-78.7	-	144.8 mg g^{-1}	-	[93]
FRP	10.0-2000.0 ng L^{-1}	85.02-102.98	3.91	4.32, 4.13 mg g^{-1}	9	[92]
AGET ATRP	0.002-0.1 mmol L^{-1}	>85	1.60	2350	60	[94]
FRP	20-2000 ng L^{-1}	76.3-94.2	9.4	307.8	-	[103]
FRP	50-1000	75.6-108.9	26.06	187	30	[89]
RAFT	0.1-100	83.1-103.1	22.6	-	60	[28]
FRP	0.25-10	75.2-104.9	33.46	50 mg g^{-1}	80	[101]
FRP	0.05-5.0 ng L^{-1}	80.2-116	67.99	-	-	[104]
FRP	0.25-25	88.3-99.1	-	146.5, 190.1 mg g^{-1}	15	[99]
FRP	0.08-0.18 ng g^{-1}	76.2-95.8	-	29.7, 135.9	20	[95]
FRP	0.5-125 ng g^{-1}	72.8-96.5	5.3	116.1	-	[105]
FRP	10-1000	71.6-90.7	-	70.71, 139.88	5	[100]
FRP	0.05-10 μg g^{-1}	82.5-111.8	3.2	94.1 mg g^{-1}	5	[96]
FRP	10-1000	86.5-91.5	2.31	100.51, 305.72	7	[97]
FRP	0.05-100.0 mg L^{-1}	82.7-88.5	30.51	31.07	30	[98]

AA acrylic acid, *AIBN* 2,2-azobisisobutyronitrile, *AGET ATRP* activator generated by electron transfer atom transfer radical polymerization, *CAP* chloramphenicol, *CCNs* carboxylated cellulose nanocrystals, *CS* chitosan, *DAD* diode array detection, *DVB* divinylbenzene, *EDA* ethylenediamine, *EGDMA* ethylene glycol dimethacrylate, *ERY* erythromycin, *FF* florfenicol, *FRP* free-radical polymerization, *GMA* glycidyl methacrylate, *HPLC* high-performance liquid chromatography, *LC* liquid chromatography, *LOD* limit of detection, *MAA* methacrylic acid, *MCNT* magnetic carbon nanotube, *MMA* methyl methacrylate, *MMWCNT* magnetic multiwalled carbon nanotube, *MPS* 3-(methacryloxy)propyl trimethoxysilane, *MS* mass spectrometry, *m-SiO_2-V* vinyl-grafted Fe_3O_4@SiO_2, *OA* oleic acid, *OFX* ofloxacin, O*TC* oxytetracycline, *PENV* penicillin V potassium, *PMMA* polymethyl methacrylate, *POSS* polyheral oligomeric silsesquioxanes, *RAFT* reversible addition fragmentation chain transfer, *SMD* sulfamethoxydiazine, *SMX* sulfamethoxazole, *SMZ* sulfamethazine, *TCT* chlortetracycline, *TRIM* trimethylolpropane trimethacrylate, *TTCA* *s*-1-dodecyl-*s*′-(α,α′-dimethyl-α″-aceticacid, *UFLC* ultra-fast liquid chromatography-tandem mass spectrometry , *2-VP* 2-vinylpyridine, *VTMOS* vinyltrimethoxysilane

had lower LODs (0.088–0.59 ng L^{-1}) and satisfactory recoveries (80.2–116%) for the detection of 12 fluoroquinolones in river water.

The practical concentrations of antibiotics are usually low (nanogram per liter level) in environmental samples. When these samples are treated with synthesized MMIP materials, possible template leakage may introduce error into the detection, which is still a big problem that needs to be overcome. Use of a dummy template (molecules sharing a similar structure with the target analytes) has been reported as a good way to solve the template leakage problem, which will be discussed in later sections. However, efforts still need to be made to find suitable dummy templates for different antibiotics.

Metal ions

The synthesis procedures for magnetic ion-imprinted polymers (IIPs) are presented schematically in Fig. 3. Differently from MIPs targeting organic molecules, the binding between the polymer and the metal ions is mainly through electrostatic or coordination interaction. Hence, ligands (or chelating agents) are added to the polymerization system because common monomers have limited combining capability. Examples of metal ions and their corresponding chelating agents are summarized in Fig. 4. Moreover, the selectivity for the target ion is a vital parameter with regard to the feasibility of the IIP, for the concentrations of some interfering ions might be more than 100 times higher than those of the target analytes.

Aiming at a selective extraction of Pb(II) ions, Fayazi et al. [110] synthesized a novel magnetic IIP by FRP using 4-vinylpyridine as the monomer, EGDMA as the cross-linker, 2,2-azobisisobutyronitrile as the initiator, and 2,3,5,6-tetra (2-pyridyl)pyrazine as the chelating agent to coordinate with Pb(II). A low LOD (2.4 ng L^{-1}), a wide linear range (0.015–0.25 ng L^{-1}), and high maximum adsorption capacity (48.1 mg g^{-1}) were obtained by the coupling of DSPE with detection by graphite furnace atomic absorption spectroscopy. Good recoveries (96.3–103.0%) were obtained in the mixing solutions containing 16 kinds of interfering ions of 500–5000 times higher concentration, which indicated that the material exhibited excellent selectivity. In work reported by Sayar et al. [113], 4-(vinylamino)pyridine-2,6-dicarboxylic acid was firstly synthesized to act as the coordination ligand as well as the functional monomer. The method was applied for detection in some environmental samples, and Pb(II) was found in soil samples. Other studies aiming at detection of lead [106, 109, 114] were also reported in recent years (Table 3).

Sol–gel polymerization was used to prepare magnetic mesoporous silica imprinted with Cd(II) ion for extraction of trace

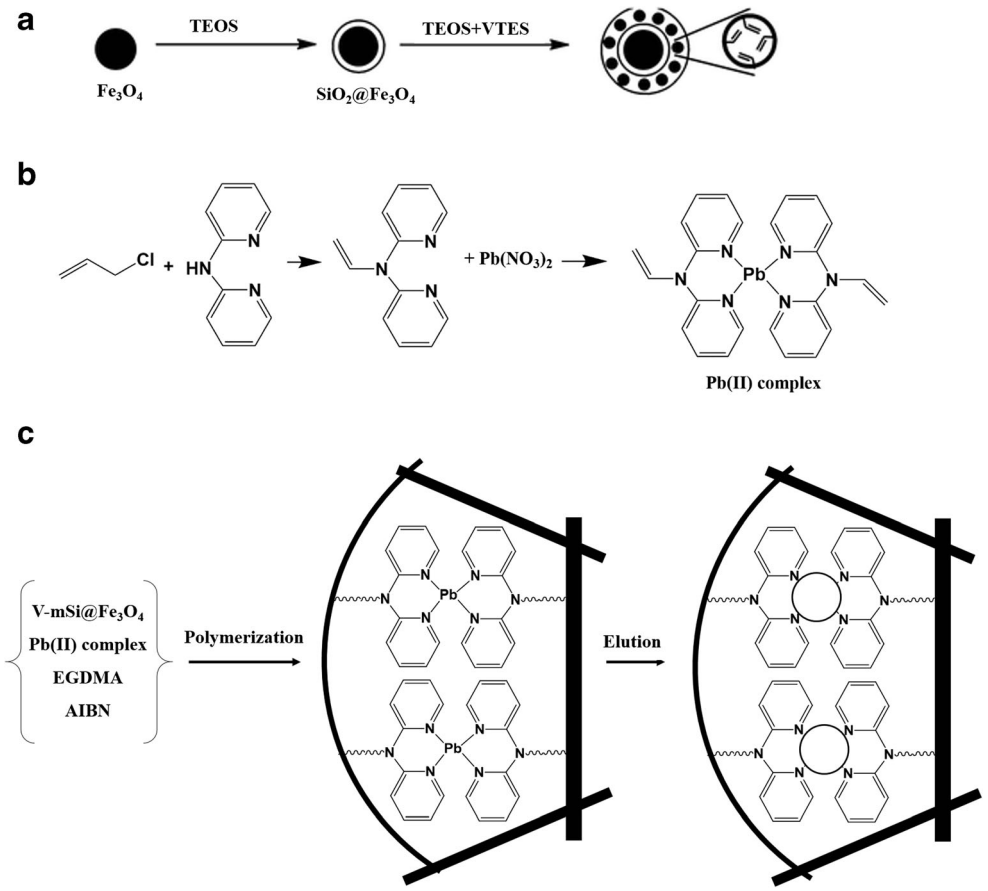

Fig. 3 The synthesis procedures for metal-ion-imprinted magnetic molecularly imprinted polymers: **a** the preparation of vinyl-modified silica coated magnetic nanoparticles (V-mSi@Fe_3O_4), **b** the formation of the metal ion and ligand/chelating agent complex, and **c** polymerization and template elution. AIBN 2,2-azobisisobutyronitrile, EGDMA ethylene glycol dimethacrylate, TEOS tetraethoxysilane, VTES allyl trimethoxysilane. (From [106], copyright 2012 Springer)

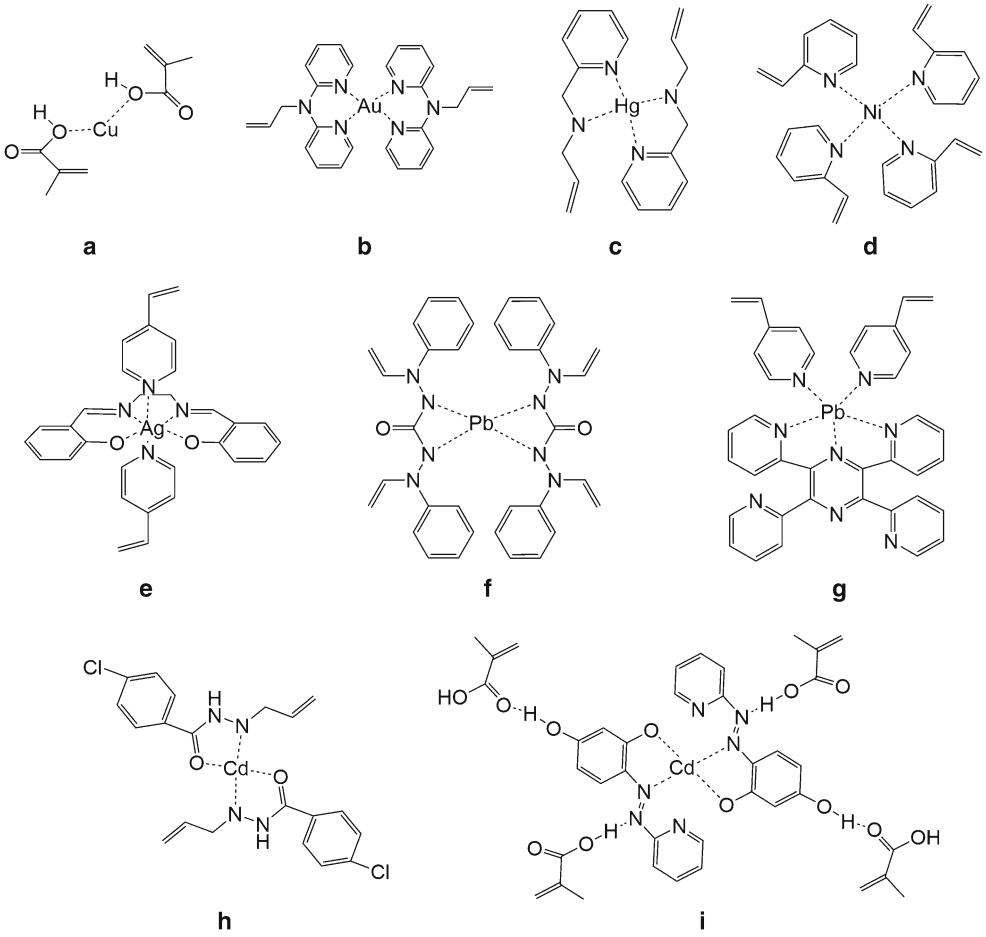

Fig. 4 Examples of metal ions and their chelating agents used to synthesize ion-imprinted magnetic molecularly imprinted polymers obtained in **a** [7], **b** [19], **c** [21], **d** [107], **e** [108], **f** [109], **g** [110], **h** [111], and **i** [112]

cadmium in real samples [41], including environmental water, human hair, and rice. The maximum adsorption amount was 32.9 mg g^{-1} and a lower LOD (6.1 ng L^{-1}) was obtained compared with other studies [106, 112], probably because of the high water compatibility of silica. However, as mentioned before, silica polymers with a rigid structure sometimes retard the mass transfer, so in some cases magnetic IIPs prepared by the sol–gel method [41, 116] exhibit much longer equilibrium times than those magnetic IIPs obtained through other MITs[111, 112].

Liu et al. [7] used another polymerization method, RAFT, in the fabrication of an IIP layer on the surface of magnetic mesoporous silica, and a monodisperse layer was obtained. The material exhibited much higher binding capacity (210 mg g^{-1}) than the material synthesized by He et al. [116], and showed superiority as a solid-phase extraction sorbent for the removal of Cu(II) in real wastewater samples. Besides, other magnetic IIPs targeting different metal ions, mainly heavy metal ions such as Ag(I) [108], Hg(II) [117], U(VI) [118], V(IV) [119], and Au(I) [120], were reported (Table 3).

However, the use of magnetic IIPs in extracting metal ions still suffers from the lack of general chelating agents. It is also reported that when small molecules are used as the template, steric hindrance should be considered [121]. As the radiuses of heavy metal ions are around 1 nm, small structural changes of the chelating agent or functional monomers may also have a great impact on the imprinting, to which attention should be paid.

MMIPs in food samples

Endocrine-disrupting compounds

Estrogens are a series of low molecular weight, lipophilic, steroidal hormones that are considered to be endocrine-disrupting compounds. As the most representative ones, the natural estrone, 17β-estradiol, and estriol and the synthetic diethylstilbestrol are widely studied [122, 123] in various fields. Obtaining a comprehensive understanding of estrogens is required in some cases as their functions are complementary to each other, so multiple templates are usually used when estrogen-imprinted materials are being prepared. Gao et al. [40] reported a multitemplate MMIP for the detection of 17β-estradiol, estriol, and diethylstilbestrol. Although the absorption capacities were slightly lower than those of single-template MIPs [122, 123], the method was able to detect these three major estrogens at the same time. In addition, the method showed good analytical performances (LODs

Table 3 Application of magnetic molecularly imprinted polymers in the sample preparation procedures for heavy metal ion analysis

Polymerization method	Magnetic materials	Monomer; cross-linker; initiator; template	Sample	Analyte	Analytical techniques	LODs (ng mL^{-1})	Linear range (ng mL^{-1})	Recovery (%)	Recognition capacity (mg g^{-1})	Recognition kinetics (min)	Reference
Distillation precipitation polymerization	Fe_3O_4@SiO_2-MPS	MAA; EGDMA; AIBN; Pb(II)	Water samples	Pb(II)	Colorimetry, electrochemical analysis	1	0-20	87.74-96.56	-	-	[114]
FRP	Fe_3O_4@mSiO_2-V	VDPC; EGDMA; AIBN; Pb(II)	Food samples	Pb(II)	FAAS	1.3	-	≥97.3	68.1	2	[109]
FRP	Fe_3O_4@mSiO_2-V	VDPyA; EGDMA; AIBN; Pb(II)	Milk	Pb(II)	FAAS	1.7	-	96.6-102.4	76.3	3	[106]
FRP	Fe_3O_4-V	MAA; EGDMA; AIBN; Pb(II)	Beverages	Pb(II)	FAAS	1.7 ng g^{-1}	5-200	94.6-101	51.8	4	[30]
Inverse microemulsion polymerization	Fe_3O_4	4-VP, acrylate-modified *Streptomyces platensis*; EGDMA; AIBN; Pb(II), Cd(II)	Soil, food samples	Pb(II), Cd(II)	ICP-AES	0.1, 0.08 ng g^{-1}	0.8-5000 ng g^{-1}	91.3-108.9	108, 56	-	[115]
Sol–gel polymerization	MMS	3-MPTMS; TEOS; NH_3OH; Cd(II)	Water, urine, rice	Cd(II)	GFAAS	6.1 ng L^{-1}	10-200 ng L^{-1}	89.3-116	32.9	20	[41]
Emulsion polymerization	Fe_3O_4-V	Synthesized ligand; EGDMA; AIBN; Cd(II)	Diesel oils	Cd(II)	FAAS	0.09	0.8-60	68.5-95.9	52.6	4	[111]
Sol–gel polymerization	Fe_3O_4@SiO_2	APTES; –; –; Cu(II)	Environmental water	Cu(II)	FAAS	0.3	1.0-150	98.4-101.2	-	5.5	[60]
RAFT	γ-Fe_2O_3@m-SiO_2-MPS	MAA; EGDMA; AIBN; Cu(II)	Wastewater	Cu(II)	ICP-AES	1.20	0.5-80.0	95.1-105	212.0	-	[7]
Sol–gel polymerization	MMWCNTs-SiO_2	DDTC, APTES; TEOS; –; Cu(II)	Herbal medicines	Cu(II)	FAAS	1.15	0.70-100.00	95.6-108.4	42.2	120	[116]
FRP	Fe_3O_4-V	V-Pic; EGDMA; AIBN; Hg(II)	Fish	Hg(II)	ICP-OES	0.03	-	98.2-103.2	147	-	[116]
FRP	Fe_3O_4@SiO_2	4-VP, salen; EGDMA; AIBN; Ag(I)	Water samples	Ag(I)	FAAS	50 ng L^{-1}	0.5-50.0	96.3-103.2	28.2	10	[108]

AIBN 2,2-azobisisobutyronitrile, *APTES* 3-aminopropyltriethoxysilane, *DDTC* diethyl dithiocarbamate, *EGDMA* ethylene glycol dimethacrylate, *FAAS* flame atomic absorption spectroscopy, *Fe_3O_4-V* vinyl-funtionalized Fe_3O_4, *FRP* free-radical polymerization, *GFAAS* graphite furnace atomic absorption spectroscopy, *ICP-AES* inductively coupled plasma atomic emission spectroscopy, *ICP-OES* inductively coupled plasma optical emission spectroscopy, *LOD* limit of detection, *MAA* methacrylic acid, *MMS* magnetic mesoporous silica, *MMWCNT* magnetic multiwalled carbon nanotube, *MPS* 3-(methacryloxy)propyl trimethoxysilane, *3-MPTMS* 3-mercaptopropyltrimethoxysilane, *m-SiO_2* mesoporous SiO_2, *RAFT* reversible addition fragmentation chain transfer, *salen* *N*,*N*′-bis(salicylidene) ethylenediamine, *Fe_3O_4@mSiO_2-V* vinyl functionalized mesoporous silica coated Fe_3O_4 , *TEOS* tetraethoxysilane, *VDPyA* vinyl dipyridylamine, *VDPC* diphenylcarbazide, *4-VP* 4-vinylpyridine, *V-Pic* *N*-(pyridin-2-ylmethyl)ethenamine

lower than 0.27 ng mL^{-1}) by the coupling with HPLC–UV detection.

Phenolic disruptors are also worrying endocrine-disrupting compounds, among which BPA is a representative. Liu et al. [61] applied an efficient method, si-ATRP, in synthesizing a core–shell MMIP. The nanoparticles served as the sorbent in DSPE, and then the eluent was analyzed by reversed-phase HPLC–UV detection. Finally, a low LOD (86.3 ng L^{-1}) and a wide linear range (0.005–0.4 μmol L^{-1}) were obtained. However, the adsorption amount (about 16 mg g^{-1}) was relatively low compared with that of other MMIPs (Table 4). Another core–shell MMIP particle [128], with an extremely high extraction amount (390 mg g^{-1}), was reported; this was prepared with 4-vinylpyridine as the functional monomer rather than 2-vinylpyridine [61]. The effect of functional monomers on the imprinting is worth further investigation. Furthermore, the imprinting factor (IF; the partition coefficient of the MIP in solution divided by the partition coefficient of the nonimprinted polymer) of BPA-imprinted materials is relatively low (about 1.5) [128, 129, 131]. It is hoped that the performance of BPA-imprinted materials will be improved by increase of the selectivity.

Additives and toxins

The detection of common additives or toxins in food samples is also a hot research topic among the applications of MMIPs. Liu et al. [42] synthesized a typical MMIP material by FRP to determine trace-level rhodamine B, which is a water-soluble dye, in wine samples. Experimental details can be found in Table 5. The MMIP particles served as sorbents in DSPE, which was followed by fluorospectrophotometry. To obtain more accessible binding sites, Su et al. [134] introduced surface imprinting technology to MMIP fabrication, and a core–shell MMIP with much higher saturated adsorption amount (104.6 mg g^{-1}) was obtained, while the value of MMIPs obtained by Liu was only 2.35 mg g^{-1} [42].

RAFT is another ideal method to prepare surface imprinting materials. Xie et al. [136] applied RAFT and obtained uniform core–shell MMIP nanoparticles for the detection of Sudan dyes in chili powder samples. The IF (8.58) was much higher than that of another core-shell MMIP obtained by traditional FRP (IF of 2.68–3.01) [135], whereas their extraction capacities were almost the same. In other words, the material obtained by Xie et al. exhibited much higher selectivity, and the other material had a higher percentage of nonspecific extraction.

Template leakage is a major problem to be solved when MIP materials are used in sample pretreatment. Residue template molecules on the MIP leak into the sample and then change the actual concentration of target analytes, which finally leads to error in detection. To overcome this drawback, dummy templates are used especially when the target analytes are highly toxic, dangerous, or hard to obtain. Aflatoxins are a group of chemically similar toxic fungal mycotoxins with five rings. On the basis of their structural features, Tan et al. [137] chose a more available molecule, 5,7-dimethoxycoumarin, as the dummy template to prepare the MMIPs through surface imprinting, using MAA and 4-vinylpyridine as the monomers and EGDMA as the cross-linker. The satisfactory IF (3.87 after optimization) demonstrated the feasibility of the dummy template imprinting technique. Although dummy template imprinting is a smart and attractive technology, optimization is required to find a suitable dummy template [138] in most situations.

MMIPs in biofluid samples

Proteins

Proteins such as antibodies and enzymes are usually used as recognition elements for diagnosis and disease therapeutics. Although MIP materials have been extensively used to selectively extract organic or inorganic substances for decades, the imprinting of macromolecules such as proteins is still a challenge. Firstly, proteins are insoluble or easily deactivated in commonly used imprinting solvents. Secondly, the conformation of a protein is highly flexible, which might lead to changes during the polymerization, so the final binding sites might not suit target analytes with native structures. In addition, the large size of proteins makes them difficult to remove from the 3D cross-linking polymer, and those binding sites far from the surface are also inaccessible. Recently, approaches for fabricating novel MIPs with higher absorption capacity for proteins, such as bovine hemoglobin [139–142], bovine serum albumin [143, 144], glycoproteins [145–147], or peptides [148, 149], have been reported.

Surface imprinting seems to be one of the most efficient strategies to ensure the accessibility of the binding sites during protein extraction. In recent work presented by Liu et al. [150], the initiator was grafted on the surface of amino-functionalized Fe_3O_4 nanoparticles, where a water-compatible layer was grown. The core–shell MMIP successfully extracted deoxyribonuclease I (31 kDa) in complex biological samples without reducing its activity. Coupling of DSPE with common fluorescent probe detection resulted in a linear working range of 10–300 ng mL^{-1} for deoxyribonuclease I being obtained. The self-assembly of dopamine is an alternative method for surface imprinting, which was used by Yin et al. [55] and Wan et al. [151] to fabricate polymers imprinted with human serum albumin and lysozyme, respectively (Fig. 5).

Although most proteins have diverse functional groups, use of various binding mechanisms (including electrostatic interaction, hydrophobic effect, hydrogen bonds, and π–π interaction) for recognition is another efficient way for successful imprinting [152]. For example, Duan et al. [153] fabricated a multiple binding site MMIP for detection of lysozyme (13.4 kDa) using ionic liquid and β-cyclodextrin-modified Fe_3O_4@dopamine/GO as the supporter to combine with the templates. Thanks

Table 4 Application of magnetic molecularly imprinted polymers in the sample preparation procedures for analysis of endocrine-disrupting compounds

Polymerization method	Magnetic materials	Monomer; cross-linker; initiator; template	Sample	Analyte	Analytical techniques	LODs (ng mL^{-1})	Linear range (ng mL^{-1})
Sol–gel polymerization	Fe_3O_4@CHO	Gelatin; E2	Water samples	E2	HPLC–UV detection	0.04	1.0-100
Self-assembly	Fe_3O_4@Nafion	DA; APS; DES	Milk powder	DES	HPLC–UV detection	0.99 ng g^{-1}	3.2-1000 ng g^{-1}
Sol–gel polymerization	Fe_3O_4@SiO_2	APTES, PTMS, TEOS; E2, E3, DES	Water samples	E2, E3, DES	HPLC–UV detection	0.27, 0.17, 0.08	1.0-100, 0.8-100, 0.3-100
FRP	Fe_3O_4@SiO_2-MA	MAA; TRIM; AIBN; EE2	Plasma	E1, E2, E3, EE2	HPLC–UV detection	0.30-0.4	1.0-25.0
FRP	Fe_3O_4@ZIF-8	ABPA; ABPA; APS; E2	Fish and pork	E1, E2, E3, EE2	SPME–HPLC	0.42-1.65 ng g^{-1}	5-1000 ng g^{-1}
FRP	Fe_3O_4@SiO_2	AA; EGDMA; AIBN; E2	Milk powder	E1, E2, E3, DES	SPME–HPLC–UV detection	1.5-5.5 ng g^{-1}	30-2000 ng g^{-1}
SFRP	Fe_3O_4@MWNTs	4-VP; TEOS; HAc; PTOP	Water samples	4-NP	HPLC	0.15	0.1-200.0 μg mL^{-1}
Miniemulsion polymerization	Fe_3O_4@MAPS	2-VP; EGDMA; AIBN; BPA	Water, milk	BPA	HPLC–UV detection	0.014, 0.16	0.1-40, 1.0-200
Sol–gel polymerization	Fe_3O_4@SiO_2-NH_2	TEOS, PTMS; BPA	Milk samples	BPA	HPLC–UV–vis detection	4.70-10.5 ng g^{-1}	-
si-ATRP	Fe_3O_4@PS@Br	4-VP; EDMA; CuBr; BPA	Tap water	BPA	RP-HPLC–UV detection	86.3 ng L^{-1}	0.005-0.4 μmol L^{-1}
Sol–gel polymerization	Fe_3O_4@SiO_2	BPAF-Si, TEOS; HAc; BPA	water samples, orange juice	BPA	HPLC–UV detection	0.3	50-1000

Polymerization method	Recovery (%)	Saturation magnetization (emu g^{-1})	Recognition capacity (mg g^{-1})	Recognition kinetics (min)	IF	Reference
Sol–gel polymerization	88.3-99.1	50.10	12.87	30	5.30	[122]
Self-assembly	85.5-105.2	63.01	9.74	20	2.63	[123]
Sol–gel polymerization	92.3-98.6	50.15	3.74, 6.02, 6.89	4	3.78, 5.14, 2.91	[40]
FRP	87.8-95.9	7.78	330.6 μmol g^{-1}	20	-	[124]
FRP	73.8-96.7	35.71	-	15	-	[125]
FRP	81.5-96.6	39.68	-	20	2.45-4.04	[126]
SFRP	88.6-98.1	26.52	52.4	20	3.22	[127]
Miniemulsion polymerization	89-106, 95-101	18	390	5	1.44	[128]
Sol–gel polymerization	85.2-98.6	-	40.2	30	1.6	[129]
si-ATRP	90.5-103.7	25.2	71.4 μmol g^{-1}	30	1.48	[61]
Sol–gel polymerization	95.0-106.2, 93.3-100.0	37.75	25.93 μmol g^{-1}	2	-	[130]

AA acrylic acid, *ABPA* 3-aminobenzeneboronicacid, *AIBN* 2,2-azobisisobutyronitrile, *APS* ammonium persulfate, *APTES* 3-aminopropyltriethoxysilane, *BPA* bisphenol A, *BPAF-Si* 2,2'-bis(4-hydroxyphenyl)-hexafluoropropane trimethylsilane, *DA* dopamine, *DES* diethylstilbestrol, *E1* estrone, *E2* 17β-estradiol, *E3* estriol, *EDMA* ethylene dimethacrylate, *EE2* 17α-ethynylestradiol, *EGDMA* ethylene glycol dimethacrylate, *FRP* free-radical polymerization, *HPLC* high-performance liquid chromatography, *IF* imprinting factor, *LOD* limit of detection, *MA* methyl acrylate, *MAA* methacrylic acid, *MPS* 3-(methacryloxy)propyl trimethoxysilane, *MWNT* multiwalled nanotube, *4-NP* 4-nitrophenol, *PTMS* phenyltrimethoxysilane, *PTOP* 4-tert-octylphenol, *RP* reversed phase, *si-ATRP* surface-initiated atom transfer radical polymerization, *SPME* solid-phase microextraction, *TEOS* tetraethoxysilane, *TRIM* trimethylolpropane trimethacrylate, *2-VP* 2-vinylpyridine, *4-VP* 4-vinylpyridine

Table 5 Application of magnetic molecularly imprinted polymers in the sample preparation procedures for analysis of additives in food

Polymerization method	Magnetic materials	Monomer; cross-linker; initiator; template	Sample	Analyte	Analytical techniques	LODs (ng mL^{-1})	Linear range (ng mL^{-1})
FRP	MCNT	MAA; EGDMA; AIBN; melamine	Milk powder	Melamine	HPLC–MS/MS	0.75 μg g^{-1}	2.5-250 μg g^{-1}
FRP	Fe_3O_4@OA	MAA; EGDMA; AIBN; melamine	Milk	Melamine	HPLC–MS/MS	2.6	10-1000
FRP	Fe_3O_4@OA	MAA; TRIM; AIBN; RhB	Wine samples	RhB	UV–vis detection	1.05	40-1400
FRP	Fe_3O_4@SiO_2-NH_2	AA; EGDMA; AIBN; RhB	Food samples	RhB	HPLC–UV–vis detection	3.4	100-8000
FRP	GO-Fe_3O_4	AA; EGDMA; AIBN; propionamide	Foods	Acrylamide	HPLC–UV detection	15 ng g^{-1}	-
FRP	Fe_3O_4@SiO_2	MAA; EGDMA; AIBN; Sudan IV	Chili powder samples	Sudan dyes (I–IV)	HPLC	1.6-6.2	25-5000
RAFT	Fe_3O_4@SiO_2-Cl	MAA; EGDMA; AIBN; Sudan I	Chili powder samples	Sudan dyes (I–IV)	HPLC–UV detection	1.8-5.7	10-10,000 (I), 20-10,000 (II–IV)

Polymerization method	Recovery (%)	Saturation magnetization (emu g^{-1})	Recognition capacity (mg g^{-1})	Recognition kinetics (min)	IF	Reference
FRP	88.6-92.1	11.57	43.82	15	-	[132]
FRP	88.0-95.8	8.7	189.39	5	3.08	[133]
FRP	75.56-81.88	-	2.35	30	1.5	[42]
FRP	78.47-101.6	21.2	104.6	30	1.88	[134]
FRP	86.7-94.3	10.8	3.68	30	2.83	[55]
FRP	79.9-87.3	18.17	42.30	10	2.68-3.01	[135]
RAFT	74.1-93.3	18.49	-	20	8.58	[136]

AA acrylic acid, *AIBN* 2,2-azobisisobutyronitrile, *EGDMA* ethylene glycol dimethacrylate, *FRP* free-radical polymerization, *GO* graphene oxide, *HPLC* high-performance liquid chromatography, *IF* imprinting factor, *LOD* limit of detection, *MAA* methacrylic acid, *MCNT* magnetic carbon nanotube, *MS* mass spectrometry, *OA* oleic acid, *RAFT* reversible addition fragmentation chain transfer, *RhB* rhodamine B, *TRIM* trimethylolpropane trimethacrylate

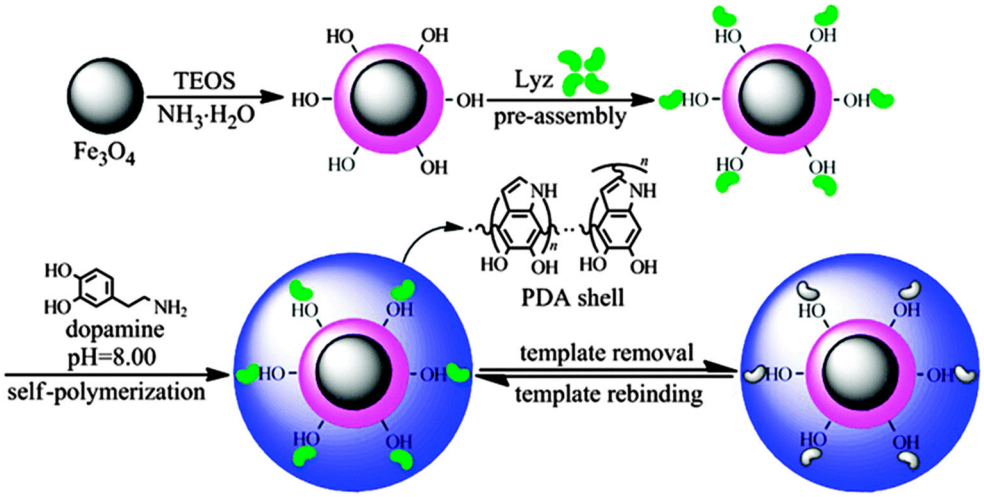

Fig. 5 Imprinting of silica-modified Fe_3O_4 nanoparticles with lysozyme (Lyz) through the self-assembly of dopamine [151]. PDA polydopamine, TEOS tetraethoxysilane. (From [151], copyright 2015 Royal Society of Chemistry)

to the multiple interaction, the MMIP materials exhibited high adsorption capacity (101 mg g^{-1}) and fast kinetics (equilibrium reached within 10 min), so the method had an extremely low LOD (0.3 ng L^{-1}) and a wide linear range (1.0–80 ng L^{-1}) by coupling with chemiluminescence detection.

The problem caused by structure flexibility of proteins is waiting to be solved, especially now that more and more evidence shows that structural changes happen during attachment of the protein to a sorbent [152]. Rather than the use of the whole molecule as a template, epitope imprinting technology using a specific portion of protein for imprinting was developed. Tan et al. [154] used a short exposed fragment peptide (epitope) of angiotensin I and angiotensin II as the template to fabricate surface-imprinted material for extraction of angiotensin I and angiotensin II. This method overcame the steric hindrance of macromolecules, such that high adsorption capacities (78.2 and 74.0 mg g^{-1}) for angiotensin I and angiotensin II as well as low LODs (0.07 and 0.06 ng mL^{-1}) of the method were obtained (Fig. 6).

Pharmaceuticals

The determination of pharmaceuticals and their metabolites is another hot topic in biofluid analysis. Differently from proteins, problems caused by size no longer occur when imprinted polymers are prepared for detection of pharmaceuticals. However, to meet the requirement of effective detection of them in biofluids, especially in blood, plasma, serum, and urine, efforts are still needed.

For example, some drugs have a short lifetime in the body, so a fast and accurate analysis method is vital in clinical detection or monitoring. Tramadol is a typical analgesic, the half-life ($t_{1/2}$) of which is about 9 h. Madrakian et al. [155] developed a rapid and selective method based on MMIPs for tramadol determination in human urine samples. For better recognition, an aminoimide monomer was firstly synthesized to from a tight complex with the templates. The LOD and linear range of the method were 1.5 ng mL^{-1} and 3.0–200.0 ng mL^{-1}, respectively, with an extraction duration of only 25 min. Another analgesic drug, morphine ($t_{1/2}$ < 3 h), was determined by Kolaei et al. [156], and the extraction took only 8 min with the synthesized multiwalled-CNT-supported MMIP.

Determining the metabolite levels of a drug is also crucial in effect evaluation and pharmacology exploration. Yang et al. [157] tried to apply MMIPs in the identification of metabolites of *Polygonum cuspodatum* in rat plasma. As expected, two MMIPs, a polydatin-imprinted one and an emodin-8-*O*-β-D-glucoside-imprinted one, showed different affinities for different groups of metabolites. The former exhibited good extraction capacity for stilbenoid metabolites, whereas the latter exhibited higher affinity for anthraquinone metabolites. Compared with traditional methods, the matrix effect was obviously lowered by the coupling of DSPE with liquid chromatography–quadrupole time-of-flight mass spectrometry. The successful application of this method demonstrated the feasibility of using MMIPs in metabolite enrichment or profiling.

Summary and future prospects

Fast, selective, and sensitive analytical methods are urgently needed in real sample analysis. Conventional solid-phase extraction sorbents require tedious collection procedures (such as filtration and centrifugation) and lack selectivity, which greatly restrict the extraction efficiency and performance, especially when the sample matrices are highly complex or the target analytes are at a low (or even trace) level. MMIPs with appealing features have frequently been used as affinity-based sorbents to overcome the aforementioned weaknesses, by simplifying the collection procedure and evidently increasing the selectivity.

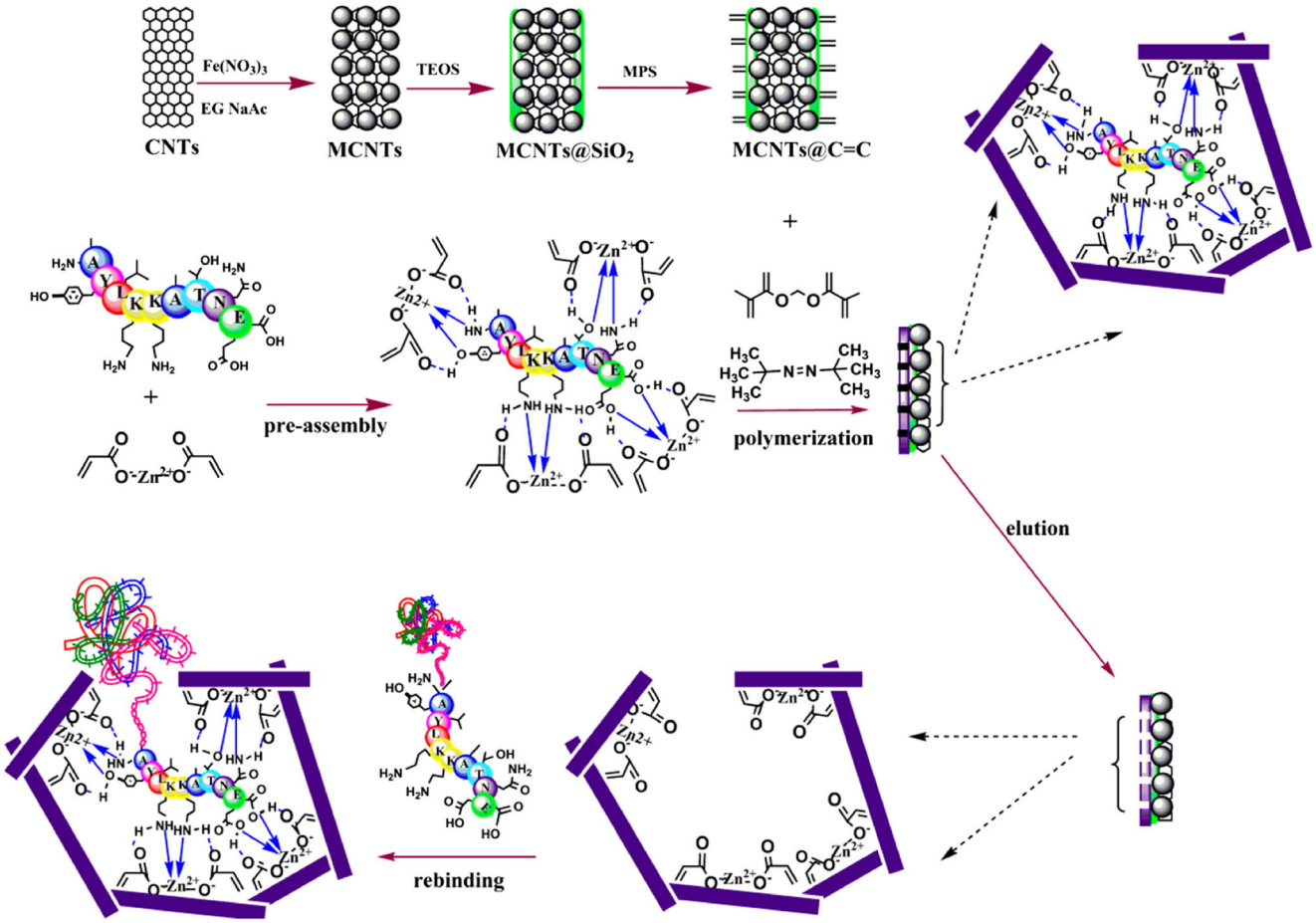

Fig. 6 Synthesis protocol for magnetic carbon nanotubes (MCNTs) coated with an epitope molecularly imprinted polymer to recognize cytochrome *c* . CNT carbon nanotube, EG ethylene glycol, MPS 3-(methacryloxy)propyl trimethoxysilane, TEOS tetraethoxysilane. (From [152], copyright 2016 American Chemical Society)

To meet various demands of detection, different MITs have been proposed [4] and various MMIPs have been developed. So far, FRP is still the most widely used MIT because of its simple fabrication and diverse options of the functional monomers [4]. However, the uncontrollable radical reaction always leads to irregular morphology, and the inner binding sites might be blocked, so the extraction amount will be limited. LCRP techniques [28, 34] and the self-assembly of polydopamine strategy [46] are ideal methods for surface imprinting or fabrication of an MIP layer with controllable thickness, in which way more accessible binding sites can be obtained. On the other hand, sol–gel silica is an attractive water-compatible MIP material, and has a mild synthesis procedure [23]. The rigid and highly cross-linked structure endows the sol–gel MIP with good stability, but at the same time hinders the mass transfer [116], which needs to be overcome. Besides increase of the accessibility of binding sites, another strategy to obtain higher extraction capacity is to increase the specific surface area of the sorbent materials, so more and more magnetic composites are being developed to act as the supporter for imprinting, such as magnetic CNTs [52], magnetic GO [55], and other porous magnetic materials [50, 58].

To obtain high selectivity for target analytes, suitable strategies should be chosen to prepare the MMIPs according to the characteristics of the templates. Other than hydrogen bonds, other binding mechanisms (including electrostatic interaction [89], chelation [110], van der Waals forces, and π–π interaction [92, 128]) could also be used to strengthen the specific binding between templates and binding sites by the design of special functional monomers [111] or addition of some interacting agents [110].

Still, MMIPs face a number of challenges during their fabrication and application. For example, a large number of MIPs are synthesized in a nonpolar solvent to avoid disruption of the hydrogen bonding between monomers and templates. However, a hydrophobic surface is formed on the materials obtained [4], which might result in the deposition of some interfering substances (such as protein fouling) [158, 159]. Although MMIPs with hydrophilic brushes [56] have been developed, the fabrication is still complicated. Developing novel MITs balancing the conflict will facilitate the efficiency and broaden the application of MMIPs. Template leakage is another challenge during the application of MMIPs in real

sample detection. Surface imprinting and dummy template imprinting are proved efficient solutions; however, effective surface imprinting techniques such as LCRP still suffer from the tedious preparation processes [7, 94], and a suitable dummy template is not always available. In addition, in most of the reported studies, only the paramagnetism of Fe_3O_4 was fully used, whereas Fe_3O_4 nanoparticles also exhibit other fascinating properties, such as the ability to generate heat under an alternating magnetic field [160] or light [161]. As temperature is a vital factor influencing both the coefficient of mass transfer and the binding constant between molecules, the introduction of the aforementioned properties could be a promising strategy to improve the performances of MMIPs.

In conclusion, the application of MMIPs opens an intriguing window for analyzing compounds in complex sample matrices, and continuous efforts should be made to develop novel MMIPs and broaden their applications.

Acknowledgements Financial support from the National Natural Science Foundation of China (grants 21377172, 21225731, 21477166, 21527813, and 21225731) and the Natural Science Foundation of Guangdong Province (grant S2013030013474) is gratefully acknowledged.

Compliance with ethical standards

Conflict of interest The authors declare that they have no competing interests.

References

1. Rios A, Zougagh M. Recent advances in magnetic nanomaterials for improving analytical processes. Trends Anal Chem. 2016;84:72–83.
2. Chen LG, Wang T, Tong J. Application of derivatized magnetic materials to the separation and the preconcentration of pollutants in water samples. Trends Anal Chem. 2011;30(7):1095–108.
3. Xie LJ, Jiang RF, Zhu F, Liu H, Ouyang GF. Application of functionalized magnetic nanoparticles in sample preparation. Anal Bioanal Chem. 2014;406(2):377–99.
4. Chen L, Wang X, Lu W, Wu X, Li J. Molecular imprinting: perspectives and applications. Chem Soc Rev. 2016;45(8):2137–211.
5. Rao HB, Lu ZW, Ge HW, Liu X, Chen BY, Zou P, et al. Electrochemical creatinine sensor based on a glassy carbon electrode modified with a molecularly imprinted polymer and a Ni@polyaniline nanocomposite. Microchim Acta. 2017;184(1):261–9.
6. Li XX, Pan JM, Dai JD, Dai XH, Xu LC, Wei X, et al. Surface molecular imprinting onto magnetic yeast composites via atom transfer radical polymerization for selective recognition of cefalexin. Chem Eng J. 2012;198:503–11.
7. Liu ZC, Hu ZY, Liu Y, Meng MJ, Ni L, Meng XG, et al. Monodisperse magnetic ion imprinted polymeric microparticles prepared by RAFT polymerization based on gamma-Fe_2O_3@meso-SiO_2 nanospheres for selective solid-phase extraction of Cu(II) in water samples. RSC Adv. 2015;5(65):52369–81.
8. Madrakian T, Afkhami A, Rahimi M, Ahmadi M, Soleimani M. Preconcentration and spectrophotometric determination of oxymetholone in the presence of its main metabolite (mestanolone) using modified maghemite nanoparticles in urine sample. Talanta. 2013;115:468–73.
9. Li XS, Xu LD, Shan YB, Yuan BF, Feng YQ. Preparation of magnetic poly(diethyl vinylphosphonate-co-ethylene glycol dimethacrylate) for the determination of chlorophenols in water samples. J Chromatogr A. 2012;1265:24–30.
10. Li YF, Qiao LQ, Li FW, Ding Y, Yang ZJ, Wang ML. Determination of multiple pesticides in fruits and vegetables using a modified quick, easy, cheap, effective, rugged and safe method with magnetic nanoparticles and gas chromatography tandem mass spectrometry. J Chromatogr A. 2014;1361:77–87.
11. Liu M, Li XY, Li JJ, Su XM, Wu ZY, Li PF, et al. Synthesis of magnetic molecularly imprinted polymers for the selective separation and determination of metronidazole in cosmetic samples. Anal Bioanal Chem. 2015;407(13):3875–80.
12. Kim J, Piao Y, Lee N, Park YI, Lee IH, Lee JH, et al. Magnetic nanocomposite spheres decorated with NiO nanoparticles for a magnetically recyclable protein separation system. Adv Mater. 2010;22(1):57–60.
13. Li X, Zhang LM, Wei XP, Li JP. A sensitive and renewable chlortoluron molecularly imprinted polymer sensor based on the gate-controlled catalytic electrooxidation of H_2O_2 on magnetic nano-NiO. Electroanalysis. 2013;25(5):1286–93.
14. Lee IS, Lee N, Park J, Kim BH, Yi YW, Kim T, et al. Ni/NiO core/shell nanoparticles for selective binding and magnetic separation of histidine-tagged proteins. J Am Chem Soc. 2006;128(33):10658–9.
15. Gu XH, Xu R, Yuan GL, Lu H, Gu BR, Xie HP. Preparation of chlorogenic acid surface-imprinted magnetic nanoparticles and their usage in separation of traditional Chinese medicine. Anal Chim Acta. 2010;675(1):64–70.
16. Lu FG, Li HJ, Sun M, Fan LL, Qiu HM, Li XJ, et al. Flow injection chemiluminescence sensor based on core-shell magnetic molecularly imprinted nanoparticles for determination of sulfadiazine. Anal Chim Acta. 2012;718:84–91.
17. Zhu WY, Jiang GY, Xu L, Li BZ, Cai QZ, Jiang HJ, et al. Facile and controllable one-step fabrication of molecularly imprinted polymer membrane by magnetic field directed self-assembly for electrochemical sensing of glutathione. Anal Chim Acta. 2015;886:37–47.
18. Shao M, Ning F, Zhao J, Wei M, Evans DG, Duan X. Preparation of Fe_3O_4@SiO_2@layered double hydroxide core-shell microspheres for magnetic separation of proteins. J Am Chem Soc. 2012;134(2):1071–7.
19. Deng Y, Qi D, Deng C, Zhang X, Zhao D. Superparamagnetic high-magnetization microspheres with an Fe_3O_4@SiO_2 core and perpendicularly aligned mesoporous SiO_2 shell for removal of microcystins. J Am Chem Soc. 2008;130(1):28–9.
20. Deng H, Li XL, Peng Q, Wang X, Chen JP, Li YD. Monodisperse magnetic single-crystal ferrite microspheres. Angew Chem Int Edit. 2005;44(18):2782–5.
21. You QP, Zhang YP, Zhang QW, Guo JF, Huang WH, Shi SY, et al. High-capacity thermo-responsive magnetic molecularly imprinted polymers for selective extraction of curcuminoids. J Chromatogr A. 2014;1354:1–8.
22. Behbahani M, Bagheri S, Amini MM, Abandansari HS, Moazami HR, Bagheri A. Application of a magnetic molecularly imprinted polymer for the selective extraction and trace detection of lamotrigine in urine and plasma samples. J Sep Sci. 2014;37(13):1610–6.
23. Lofgreen JE, Ozin GA. Controlling morphology and porosity to improve performance of molecularly imprinted sol-gel silica. Chem Soc Rev. 2014;43(3):911–33.
24. Wang XH, Fang QX, Liu SP, Chen L. Preparation of a magnetic molecularly imprinted polymer with pseudo template for rapid

simultaneous determination of cyromazine and melamine in biomatrix samples. Anal Bioanal Chem. 2012;404:1555–64.
25. Hang H, Li CX, Pan JM, Li LZ, Dai JD, Dai XH, et al. Selective separation of lambdacyhalothrin by porous/magnetic molecularly imprinted polymers prepared by Pickering emulsion polymerization. J Sep Sci. 2013;36(19):3285–94.
26. Dai JD, He JS, Xie AT, Gao L, Pan JM, Chen X, et al. Novel pitaya-inspired well-defined core–shell nanospheres with ultrathin surface imprinted nanofilm from magnetic mesoporous nanosilica for highly efficient chloramphenicol removal. Chem Eng J. 2016;284:812–22.
27. Liu LK, Cao Y, Ma PF, Qiu CX, Xu WZ, Liu H, et al. Rational design and preparation of magnetic imprinted polymers for removal of indole by molecular simulation and improved atom transfer radical polymerization. RSC Adv. 2014;4(2):605–16.
28. He YH, Huang YY, Jin YL, Liu XJ, Liu GQ, Zhao R. Well-defined nanostructured surface-imprinted polymers for highly selective magnetic separation of fluoroquinolones in human urine. ACS Appl Mater Interfaces. 2014;6(12):9634–42.
29. Men HF, Liu HQ, Zhang ZL, Huang J, Zhang J, Zhai YY, et al. Synthesis, properties and application research of atrazine Fe_3O_4@SiO_2 magnetic molecularly imprinted polymer. Environ Sci Pollut Res. 2012;19(6):2271–80.
30. Ebrahimzadeh H, Asgharinezhad AA, Moazzen E, Amini MM, Sadeghi O. A magnetic ion-imprinted polymer for lead(II) determination: A study on the adsorption of lead(II) by beverages. J Food Compos Anal. 2015;41:74–80.
31. Zhang YG, Song D, Lanni L, Shimizu KD. Importance of functional monomer dimerization in the molecular imprinting process. Macromolecules. 2010;43(15):6284–94.
32. Hu YL, Pan JL, Zhang KG, Lian HX, Li GK. Novel applications of molecularly-imprinted polymers in sample preparation. Trends Anal Chem. 2013;43:37–52.
33. Matyjaszewski K, Xia J. Atom transfer radical polymerization. Chem Rev. 2001;101(9):2921–90.
34. Liu YL, Huang YY, Liu JZ, Wang WZ, Liu GQ, Zhao R. Superparamagnetic surface molecularly imprinted nanoparticles for water-soluble pefloxacin mesylate prepared via surface initiated atom transfer radical polymerization and its application in egg sample analysis. J Chromatogr A. 2012;1246:15–21.
35. Jakubowski W, Matyjaszewski K. Activator generated by electron transfer for atom transfer radical polymerization. Macromolecules. 2005;38(10):4139–46.
36. Gonzato C, Courty M, Pasetto P, Haupt K. Magnetic molecularly imprinted polymer nanocomposites via surface-initiated RAFT polymerization. Adv Funct Mater. 2011;21(20):3947–53.
37. Li JH, Dong RC, Wang XY, Xiong H, Xu SF, Shen DZ, et al. One-pot synthesis of magnetic molecularly imprinted microspheres by RAFT precipitation polymerization for the fast and selective removal of 17 beta-estradiol. RSC Adv. 2015;5(14):10611–8.
38. Li Y, Li X, Chu J, Dong CK, Qi JY, Yuan YX. Synthesis of core-shell magnetic molecular imprinted polymer by the surface RAFT polymerization for the fast and selective removal of endocrine disrupting chemicals from aqueous solutions. Environ Pollut. 2010;158(6):2317–23.
39. Xu S, Li J, Chen L. Molecularly imprinted core-shell nanoparticles for determination of trace atrazine by reversible addition-fragmentation chain transfer surface imprinting. J Mater Chem. 2011;21(12):4346–51.
40. Gao RX, Hao Y, Zhao SQ, Zhang LL, Cui XH, Liu DC, et al. Novel magnetic multi-template molecularly imprinted polymers for specific separation and determination of three endocrine disrupting compounds simultaneously in environmental water samples. RSC Adv. 2014;4(100):56798–808.
41. Zhao BS, He M, Chen BB, Hu B. Novel ion imprinted magnetic mesoporous silica for selective magnetic solid phase extraction of trace Cd followed by graphite furnace atomic absorption spectrometry detection. Spectrochim Acta B. 2015;107:115–24.
42. Liu XY, Yu D, Yu YC, Ji SJ. Preparation of a magnetic molecularly imprinted polymer for selective recognition of rhodamine B. Appl Surf Sci. 2014;320:138–45.
43. Avnir D. Organic chemistry within ceramic matrixes: doped sol-gel materials. Acc Chem Res. 1995;28(8):328–34.
44. Yao GH, Liang RP, Huang CF, Wang Y, Qiu JD. Surface plasmon resonance sensor based on magnetic molecularly imprinted polymers amplification for pesticide recognition. Anal Chem. 2013;85(24):11944–51.
45. Xia XP, Xu ML, Wang YZ, Ran D, Yang S, Zhang M. Polydopamine-based molecular imprinting on silica-modified magnetic nanoparticles for recognition and separation of bovine hemoglobin. Analyst. 2013;138(2):651–8.
46. Li XJ, Zhou JJ, Tian L, Wang YF, Zhang BL, Zhang HP, et al. Preparation of anti-nonspecific adsorption polydopamine-based surface protein-imprinted magnetic microspheres with the assistance of 2-methacryloyloxyethyl phosphorylcholine and its application for protein recognition. Sensors Actuators B Chem. 2017;241:413–21.
47. Lee H, Dellatore SM, Miller WM, Messersmith PB. Mussel-inspired surface chemistry for multifunctional coatings. Science. 2007;318(5849):426–30.
48. Aguilar-Arteaga K, Rodriguez JA, Barrado E. Magnetic solids in analytical chemistry: a review. Anal Chim Acta. 2010;674(2):157–65.
49. Zou YL, Zhao CY, Dai JD, Zhou ZP, Pan JM, Yu P, et al. Magnetic and hydrophilic imprinted particles via ATRP at room temperature for selective separation of sulfamethazine. Colloid Polym Sci. 2014;292(2):333–42.
50. Li H, Hu X, Zhang YP, Shi SY, Jiang XY, Chen XQ. High-capacity magnetic hollow porous molecularly imprinted polymers for specific extraction of protocatechuic acid. J Chromatogr A. 2015;1404:21–7.
51. Luo J, Gao YH, Tan K, Wei W, Liu XY. Preparation of a magnetic molecularly imprinted graphene composite highly adsorbent for 4-nitrophenol in aqueous medium. ACS Sustain Chem Eng. 2016;4(6):3316–26.
52. Ma GF, Chen LG. Development of magnetic molecularly imprinted polymers based on carbon nanotubes - application for trace analysis of pyrethroids in fruit matrices. J Chromatogr A. 2014;1329:1–9.
53. Zhao Y-G, Zhou L-X, Pan S-D, Zhan P-P, Chen X-H, Jin M-C. Fast determination of 22 sulfonamides from chicken breast muscle using core–shell nanoring amino-functionalized superparamagnetic molecularly imprinted polymer followed by liquid chromatography-tandem mass spectrometry. J Chromatogr A. 2014;1345:17–28.
54. Ma W, Dai JD, Dai XH, Da ZL, Yan YS. Core-shell molecularly imprinted polymers based on magnetic chitosan microspheres for chloramphenicol selective adsorption. Monatsh Chem. 2015;146(3):465–74.
55. Yin YL, Yan L, Zhang ZH, Wang J. Magnetic molecularly imprinted polydopamine nanolayer on multiwalled carbon nanotubes surface for protein capture. Talanta. 2015;144:671–9.
56. Dai JD, Zhou ZP, Zou YL, Wei X, Dai XH, Li CX, et al. Surface imprinted core-shell nanorod with ultrathin water-compatible polymer brushes for specific recognition and adsorption of sulfamethazine in water medium. J Appl Polym Sci. 2014;131(19):40854.
57. Yan L, Yin YL, Lv PP, Zhang ZH, Wang J, Long F. Synthesis and application of novel 3D magnetic chlorogenic acid imprinted polymers based on a graphene carbon nanotube composite. J Agric Food Chem. 2016;64(15):3091–100.

58. Chambers SD, Holcombe TW, Svec F, JMJ F. Porous polymer monoliths functionalized through copolymerization of a C_{60} fullerene-containing methacrylate monomer for highly efficient separations of small molecules. Anal Chem. 2011;83:9478–84.
59. Ansell RJ, Mosbach K. Magnetic molecularly imprinted polymer beads for drug radioligand binding assay. Analyst. 1998;123(7): 1611–6.
60. Luo XB, Huang YN, Deng F, Luo SL, Zhan YC, Shu HY, et al. A magnetic copper(II)-imprinted polymer for the selective enrichment of trace copper(II) ions in environmental water. Microchim Acta. 2012;179(3-4):283–9.
61. Liu J, Wang W, Xie Y, Huang Y, Liu Y, Liu X, et al. A novel polychloromethylstyrene coated superparamagnetic surface molecularly imprinted core-shell nanoparticle for bisphenol A. J Mater Chem. 2011;21(25):9232–8.
62. Xiao DL, Wang CX, Dai H, Peng J, He J, Zhang K, et al. Applications of magnetic surface imprinted materials for solid phase extraction of levofloxacin in serum samples. J Mol Recognit. 2015;28(5):277–84.
63. Xiao D, Dramou P, Xiong N, He H, Li H, Yuan D, et al. Development of novel molecularly imprinted magnetic solid-phase extraction materials based on magnetic carbon nanotubes and their application for the determination of gatifloxacin in serum samples coupled with high performance liquid chromatography. J Chromatogr A. 2013;1274:44–53.
64. Ma P, Zhou ZP, Dai JD, Qin L, Ye XB, Chen X, et al. A biomimetic Setaria viridis-inspired imprinted nanoadsorbent: green synthesis and application to the highly selective and fast removal of sulfamethazine. RSC Adv. 2016;6(12):9619–30.
65. Ning FJ, Qiu TT, Wang Q, Peng HL, Li YB, Wu XQ, et al. Dummy-surface molecularly imprinted polymers on magnetic graphene oxide for rapid and selective quantification of acrylamide in heat-processed (including fried) foods. Food Chem. 2017;221:1797–804.
66. Zhao YG, Chen XH, Pan SD, Zhu H, Shen HY, Jin MC. Self-assembly of a surface bisphenol A-imprinted core-shell nanoring amino-functionalized superparamagnetic polymer. J Mater Chem A. 2013;1(38):11648–58.
67. Rios A, Zougagh M, Bouri M. Magnetic (nano)materials as an useful tool for sample preparation in analytical methods. A review. Anal Methods. 2013;5:4558–73.
68. Kubo T, Otsuka K. Recent progress in molecularly imprinted media by new preparation concepts and methodological approaches for selective separation of targeting compounds. Trends Anal Chem. 2016;81:102–9.
69. Whitcombe MJ, Rodriguez ME, Villar P, Vulfson EN. A new method for the introduction of recognition site functionality into polymers prepared by molecular imprinting: synthesis and characterization of polymeric receptors for cholesterol. J Am Chem Soc. 1995;117(27):7105–11.
70. Ki CD, Oh C, Oh SG, Chang JY. The use of a thermally reversible bond for molecular imprinting of silica spheres. J Am Chem Soc. 2002;124:14838–9.
71. Qiao FX, Row KH, Wang MG. Water-compatible magnetic imprinted microspheres for rapid separation and determination of triazine herbicides in environmental water. J Chromatogr B. 2014;957:84–9.
72. Zhang Y, Liu RJ, Hu YL, Li G. Microwave heating in preparation of magnetic molecularly imprinted polymer beads for trace triazines analysis in complicated samples. Anal Chem. 2009;81(3): 967–76.
73. Cho CMH, Mulchandani A, Chen W. Bacterial cell surface display of organophosphorus hydrolase for selective screening of improved hydrolysis of organophosphate nerve agents. Appl Environ Microbiol. 2002;68(4):2026–30.
74. Miao SS, Wu MS, Zuo HG, Jiang C, Jin SF, Lu YC, et al. Core-shell magnetic molecularly imprinted polymers as sorbent for sulfonylurea herbicide residues. J Agric Food Chem. 2015;63(14): 3634–45.
75. Pan JM, Zhu WJ, Dai XH, Yan XS, Gan MY, Li LZ, et al. Magnetic molecularly imprinted microcapsules derived from Pickering emulsion polymerization and their novel adsorption characteristics for lambda-cyhalothrin. RSC Adv. 2014;4(9): 4435–43.
76. Liu CB, Song ZL, Pan JM, Wei X, Gao L, Yan YS, et al. Molecular imprinting in fluorescent particle stabilized Pickering emulsion for selective and sensitive optosensing of lambda-cyhalothrin. J Phys Chem C. 2013;117(20):10445–53.77.
77. Hu YL, Liu RJ, Zhang Y, Li GK. Improvement of extraction capability of magnetic molecularly imprinted polymer beads in aqueous media via dual-phase solvent system. Talanta. 2009;79 (3):576–82.
78. Zare F, Ghaedi M, Daneshfar A, Ostovan A. Magnetic molecularly imprinted polymer for the efficient and selective preconcentration of diazinon before its determination by high-performance liquid chromatography. J Sep Sci. 2015;38(16): 2797–803.
79. Bazmandegan-Shamili A, Dadfarnia S, Shabani AMH, Saeidi M, Moghadam MR. High-performance liquid chromatographic determination of diazinon after its magnetic dispersive solid-phase microextraction using magnetic molecularly imprinted polymer. Food Anal Methods. 2016;9(9):2621–30.
80. Ma GF, Chen LG. Determination of chlorpyrifos in rice based on magnetic molecularly imprinted polymers coupled with high-performance liquid chromatography. Food Anal Methods. 2014;7(2):377–88.
81. Xu SY, Guo CJ, Li YX, Yu ZR, Wei CH, Tang YW. Methyl parathion imprinted polymer nanoshell coated on the magnetic nanocore for selective recognition and fast adsorption and separation in soils. J Hazard Mater. 2014;264:34–41.
82. You XX, Chen LG. Analysis of sulfonylurea herbicides in grain samples using molecularly imprinted polymers on the surface of magnetic carbon nanotubes by extraction coupled with HPLC. Anal Methods. 2016;8(5):1003–12.
83. Lerma-Garcia MJ, Zougagh M, Rios A. Magnetic molecular imprint-based extraction of sulfonylurea herbicides and their determination by capillary liquid chromatography. Microchim Acta. 2013;180(5-6):363–70.
84. Gao L, Wang JX, Li XY, Yan YS, Li CX, Pan JM. A core-shell surface magnetic molecularly imprinted polymers with fluorescence for lambda-cyhalothrin selective recognition. Anal Bioanal Chem. 2014;406(28):7213–20.
85. Li SH, Xu MZ, Wu XJ, Luo JH. Synergetic recognition and separation of kelthane and pyridaben base on magnetic molecularly imprinted polymer nanospheres. J Sep Sci. 2016;39(20):4019–26.
86. Li SH, Wu XJ, Zhang Q, Li PP. Synergetic dual recognition and separation of the fungicide carbendazim by using magnetic nanoparticles carrying a molecularly imprinted polymer and immobilized beta-cyclodextrin. Microchim Acta. 2016;183(4): 1433–9.
87. Gao L, Chen LG, Li XW. Magnetic molecularly imprinted polymers based on carbon nanotubes for extraction of carbamates. Microchim Acta. 2015;182(3-4):781–7.
88. Cheng XL, Yan HY, Wang XL, Sun N, Qiao XQ. Vortex-assisted magnetic dispersive solid-phase microextraction for rapid screening and recognition of dicofol residues in tea products. Food Chem. 2014;162:104–9.
89. Qiao FX, Gao MM, Yan HY. Molecularly imprinted ionic liquid magnetic microspheres for the rapid isolation of organochlorine pesticides in environmental water. J Sep Sci. 2016;39(7):1310–5.

90. Masoumi A, Hemmati K, Ghaemy M. Recognition and selective adsorption of pesticides by superparamagnetic molecularly imprinted polymer nanospheres. RSC Adv. 2016;6(55):49401–10.
91. Moreno-Bondi MC, Marazuela MD, Herranz S, Rodriguez E. An overview of sample preparation procedures for LC-MS multiclass antibiotic determination in environmental and food samples. Anal Bioanal Chem. 2009;395(4):921–46.
92. Qin SL, Su LQ, Wang P, Gao Y. Rapid and selective extraction of multiple sulfonamides from aqueous samples based on Fe_3O_4-chitosan molecularly imprinted polymers. Anal Methods. 2015;7(20):8704–13.
93. Chen HY, Zhang YQ, Gao B, Xu Y, Zhao Q, Hou J, et al. Fast determination of sulfonamides and their acetylated metabolites from environmental water based on magnetic molecularly imprinted polymers. Environ Sci Pollut Res. 2013;20(12):8567–78.
94. Xu LC, Pan JM, Dai JD, Cao ZJ, Hang H, Li XX, et al. Magnetic ZnO surface-imprinted polymers prepared by ARGET ATRP and the application for antibiotics selective recognition. RSC Adv. 2012;2(13):5571–9.
95. Kong JH, Wang YZ, Nie C, Ran D, Jia XP. Preparation of magnetic mixed-templates molecularly imprinted polymer for the separation of tetracycline antibiotics from egg and honey samples. Anal Methods. 2012;4(4):1005–11.
96. Zhou YS, Zhou TT, Jin H, Jing T, Song B, Zhou YK, et al. Rapid and selective extraction of multiple macrolide antibiotics in foodstuff samples based on magnetic molecularly imprinted polymers. Talanta. 2015;137:1–10.
97. Ding J, Zhang FS, Zhang XP, Wang L, Wang CJ, Zhao Q, et al. Determination of roxithromycin from human plasma samples based on magnetic surface molecularly imprinted polymers followed by liquid chromatography-tandem mass spectromer. J Chromatogr B. 2016;1021:221–8.
98. Rao W, Cai R, Zhang ZH, Yin YL, Long F, Fu XX. Fast separation and determination of erythromycin with magnetic imprinted solid extraction coupled with high performance liquid chromatography. RSC Adv. 2014;4(36):18503–11.
99. Wei SL, Li JW, Liu Y, Ma JK. Development of magnetic molecularly imprinted polymers with double templates for the rapid and selective determination of amphenicol antibiotics in water, blood, and egg samples. J Chromatogr A. 2016;1473:19–27.
100. Zhang X, Chen L, Xu Y, Wang H, Zeng Q, Zhao Q, et al. Determination of beta-lactam antibiotics in milk based on magnetic molecularly imprinted polymer extraction coupled with liquid chromatography-tandem mass spectrometry. J Chromatogr B. 2010;878(32):3421–6.
101. Wang YF, Wang YG, Ouyang XK, Yang LY. Surface-imprinted magnetic carboxylated cellulose nanocrystals for the highly selective extraction of six fluoroquinolones from egg samples. ACS Appl Mater Interfaces. 2017;9(2):1759–69.
102. Xiao DL, Dramou P, Xiong NQ, He H, Yuan DH, Dai H, et al. Preparation of molecularly imprinted polymers on the surface of magnetic carbon nanotubes with a pseudo template for rapid simultaneous extraction of four fluoroquinolones in egg samples. Analyst. 2013;138(11):3287–96.
103. Chen LG, Zhang XP, Xu Y, Du XB, Sun X, Sun L, et al. Determination of fluoroquinolone antibiotics in environmental water samples based on magnetic molecularly imprinted polymer extraction followed by liquid chromatography-tandem mass spectrometry. Anal Chim Acta. 2010;662(1):31–8.
104. Chen XH, Zhao YG, Zhang Y, Shen HY, Pan SD, Jin MC. Ethylenediamine-functionalized superparamagnetic carbon nanotubes for magnetic molecularly imprinted polymer matrix solid-phase dispersion extraction of 12 fluoroquinolones in river water. Anal Methods. 2015;7(14):5838–46.
105. Chen L, Liu J, Zeng Q, Wang H, Yu A, Zhang H, et al. Preparation of magnetic molecularly imprinted polymer for the separation of tetracycline antibiotics from egg and tissue samples. J Chromatogr A. 2009;1216(18):3710–9.
106. Sadeghi O, Aboufazeli F, Zhad H, Karimi M, Najafi E. Determination of Pb(II) ions using novel ion-imprinted polymer magnetic nanoparticles: investigation of the relation between Pb (II) ions in cow's milk and their nutrition. Food Anal Methods. 2013;6(3):753–60.
107. Asgharinezhad AA, Jalilian N, Ebrahimzadeh H, Panjali Z. A simple and fast method based on new magnetic ion imprinted polymer nanoparticles for the selective extraction of Ni(II) ions in different food samples. RSC Adv. 2015;5(56):45510–9.
108. Kazemi E, Shabani AMH, Dadfarnia S. Synthesis and characterization of a nanomagnetic ion imprinted polymer for selective extraction of silver ions from aqueous samples. Microchim Acta. 2015;182(5-6):1025–33.
109. Aboufazeli F, Zhad H, Sadeghi O, Karimi M, Najafi E. Novel ion imprinted polymer magnetic mesoporous silica nano-particles for selective separation and determination of lead ions in food samples. Food Chem. 2013;141(4):3459–65.
110. Fayazi M, Taher MA, Afzali D, Mostafavi A, Ghanei-Motlagh M. Synthesis and application of novel ion-imprinted polymer coated magnetic multi-walled carbon nanotubes for selective solid phase extraction of lead(II) ions. Mater Sci Eng C Mater Biol Appl. 2016;60:365–73.
111. Ebrahimzadeh H, Kasaeian M, Khalilzadeh A, Moazzen E. New magnetic polymeric nanoparticles for extraction of trace cadmium ions and the determination of cadmium content in diesel oil samples. Anal Methods. 2014;6(13):4617–24.
112. Zarezade V, Behbahani M, Omidi F, Abandansari HS, Hesam G. A new magnetic tailor made polymer for separation and trace determination of cadmium ions by flame atomic absorption spectrophotometry. RSC Adv. 2016;6(105):103499–507.
113. Sayar O, Torbati NA, Saravani H, Mehrani K, Behbahani A, Zadeh HRM. A novel magnetic ion imprinted polymer for selective adsorption of trace amounts of lead(II) ions in environment samples. J Ind Eng Chem. 2014;20(5):2657–62.
114. Cui Y, Liu JQ, Hu ZJ, Xu XW, Gao HW. Well-defined surface ion-imprinted magnetic microspheres for facile onsite monitoring of lead ions at trace level in water. Anal Methods. 2012;4(10):3095–7.
115. Wei SL, Liu Y, Shao MD, Liu L, Wang HW, Liu YQ. Preparation of magnetic Pb(II) and Cd(II) ion-imprinted microspheres and their application in determining the Pb(II) and Cd(II) contents of environmental and food samples. RSC Adv. 2014;4(56):29715–23.
116. He H, Xiao DL, He J, Li H, He H, Dai H, et al. Preparation of a core-shell magnetic ion-imprinted polymer via a sol-gel process for selective extraction of Cu(II) from herbal medicines. Analyst. 2014;139(10):2459–66.
117. Najafi E, Aboufazeli F, Zhad H, Sadeghi O, Amani V. A novel magnetic ion imprinted nano-polymer for selective separation and determination of low levels of mercury(II) ions in fish samples. Food Chem. 2013;141(4):4040–5.
118. Sadeghi S, Aboobakri E. Magnetic nanoparticles with an imprinted polymer coating for the selective extraction of uranyl ions. Microchim Acta. 2012;178(1-2):89–97.
119. Aliakbari A, Amini MM, Mehrani K, Zadeh HRM. Magnetic ion imprinted polymer nanoparticles for the preconcentration of vanadium(IV) ions. Microchim Acta. 2014;181(15-16):1931–8.
120. Ebrahimzadeh H, Moazzen E, Amini MM, Sadeghi O. Novel magnetic ion imprinted polymer as a highly selective sorbent for extraction of gold ions in aqueous samples. Anal Methods. 2012;4(10):3232–7.

121. Kirsch N, Alexander C, Davies S, Whitcombe MJ. Sacrificial spacer and non-covalent routes toward the molecular imprinting of "poorly-functionalized" N-heterocycles. Anal Chim Acta. 2004;504(1):63–71.
122. Hao Y, Gao RX, Shi L, Liu DC, Tang YH, Guo ZJ. Water-compatible magnetic imprinted nanoparticles served as solid-phase extraction sorbents for selective determination of trace 17beta-estradiol in environmental water samples by liquid chromatography. J Chromatogr A. 2015;1396:7–16.
123. Qiao L, Gan N, Hu FT, Wang D, Lan HZ, Li TH, et al. Magnetic nanospheres with a molecularly imprinted shell for the preconcentration of diethylstilbestrol. Microchim Acta. 2014;181 (11-12):1341–51.
124. Wang S, Wang R, Wu X, Wang Y, Xue C, Wu J, et al. Magnetic molecularly imprinted nanoparticles based on dendritic-grafting modification for determination of estrogens in plasma samples. J Chromatogr B. 2012;905:105–12.
125. Lan HZ, Gan N, Pan DD, Hu FT, Li TH, Long NB, et al. Development of a novel magnetic molecularly imprinted polymer coating using porous zeolite imidazolate framework-8 coated magnetic iron oxide as carrier for automated solid phase microextraction of estrogens in fish and pork samples. J Chromatogr A. 2014;1365:35–44.
126. Lan HZ, Gan N, Pan DD, Hu FT, Li TH, Long NB, et al. An automated solid-phase microextraction method based on magnetic molecularly imprinted polymer as fiber coating for detection of trace estrogens in milk powder. J Chromatogr A. 2014;1331:10–8.
127. Rao W, Cai R, Yin YL, Long F, Zhang ZH. Magnetic dummy molecularly imprinted polymers based on multi-walled carbon nanotubes for rapid selective solid-phase extraction of 4-nonylphenol in aqueous samples. Talanta. 2014;128:170–6.
128. Ji YS, Yin JJ, Xu ZG, Zhao CD, Huang HY, Zhang HX, et al. Preparation of magnetic molecularly imprinted polymer for rapid determination of bisphenol A in environmental water and milk samples. Anal Bioanal Chem. 2009;395(4):1125–33.
129. Lv YK, He YD, Xiong X, Wang JZ, Wang HY, Han YM. Layer-by-layer fabrication of restricted access media-molecularly imprinted magnetic microspheres for magnetic dispersion microextraction of bisphenol A from milk samples. New J Chem. 2015;39(3):1792–9.
130. Wu X, Li YR, Zhu XL, He CY, Wang Q, Liu SR. Dummy molecularly imprinted magnetic nanoparticles for dispersive solid-phase extraction and determination of bisphenol A in water samples and orange juice. Talanta. 2017;162:57–64.
131. Wang M, She YX, Du XW, Huang YT, Shi XM, Jin MJ, et al. Determination of melamine using magnetic molecular imprinted polymers and high performance liquid chromatography. Anal Lett. 2013;46(1):120–30.
132. Zhao XY, Chen LG. Analysis of melamine in milk powder by using a magnetic molecularly imprinted polymer based on carbon nanotubes with ultra high performance liquid chromatography and tandem mass spectrometry. J Sep Sci. 2016;39(19):3775–81.
133. He D, Zhang XP, Gao B, Wang L, Zhao Q, Chen HY, et al. Preparation of magnetic molecularly imprinted polymer for the extraction of melamine from milk followed by liquid chromatography-tandem mass spectrometry. Food Control. 2014;36(1):36–41.
134. Su XM, Li XY, Li JJ, Liu M, Lei FH, Tan XC, et al. Synthesis and characterization of core-shell magnetic molecularly imprinted polymers for solid-phase extraction and determination of rhodamine B in food. Food Chem. 2015;171:292–7.
135. Piao CY, Chen LG. Separation of Sudan dyes from chilli powder by magnetic molecularly imprinted polymer. J Chromatogr A. 2012;1268:185–90.
136. Xie XY, Chen L, Pan XY, Wang SC. Synthesis of magnetic molecularly imprinted polymers by reversible addition fragmentation chain transfer strategy and its application in the Sudan dyes residue analysis. J Chromatogr A. 2015;1405:32–9.
137. Tan L, He R, Chen KC, Peng RF, Huang C, Yang R, et al. Ultra-high performance liquid chromatography combined with mass spectrometry for determination of aflatoxins using dummy molecularly imprinted polymers deposited on silica-coated magnetic nanoparticles. Microchim Acta. 2016;183(4):1469–77.
138. Urraca J, Huertas-Perez JF, Cazorla GA, Gracia-Mora J, Garcia-Campana AM, Moreno-Bondi MC. Development of magnetic molecularly imprinted polymers for selective extraction: determination of citrinin in rice samples by liquid chromatography with UV diode array detection. Anal Bioanal Chem. 2016;408(11): 3033–42.
139. Gao RX, Zhang LL, Hao Y, Cui XH, Liu DC, Zhang M, et al. One-step preparation of magnetic imprinted nanoparticles adopting dopamine-cupric ion as a co-monomer for the specific recognition of bovine hemoglobin. J Sep Sci. 2015;38(20):3568–74.
140. Zhang M, Wang YZ, Jia XP, He MZ, Xu ML, Yang S, et al. The preparation of magnetic molecularly imprinted nanoparticles for the recognition of bovine hemoglobin. Talanta. 2014;120:376–85.
141. Sun YH, Chen J, Li YQ, Li H, Zhu XH, Hu YW, et al. Bio-inspired magnetic molecularly imprinted polymers based on Pickering emulsions for selective protein recognition. New J Chem. 2016;40(10):8745–52.
142. Li YX, Chen YT, Huang L, Lou BY, Chen GN. Creating BHb-imprinted magnetic nanoparticles with multiple binding sites. Analyst. 2017;142(2):302–9.
143. Gai QQ, Qu F, Zhang T, Zhang YK. The preparation of bovine serum albumin surface-imprinted superparamagnetic polymer with the assistance of basic functional monomer and its application for protein separation. J Chromatogr A. 2011;1218(22):3489–95.
144. Chen FF, Zhao WF, Zhang JJ, Kong J. Magnetic two-dimensional molecularly imprinted materials for the recognition and separation of proteins. Phys Chem Chem Phys. 2016;18(2):718–25.
145. Bei ZJ, Chen Y, Ye J, Wang SS, Liu Z. Boronate-affinity glycan-oriented surface imprinting: a new strategy to mimic lectins for the recognition of an intact glycoprotein and its characteristic fragments. Angew Chem Int Ed. 2015;54(35):10211–5.
146. Sun LX, Lin DH, Lin GW, Wang L, Lin ZA. Click synthesis of boronic acid-functionalized molecularly imprinted silica nanoparticles with polydopamine coating for enrichment of trace glycoproteins. Anal Methods. 2015;7(23):10026–31.
147. Ma RT, Ha W, Chen J, Shi YP. Highly dispersed magnetic molecularly imprinted nanoparticles with well-defined thin film for the selective extraction of glycoprotein. J Mater Chem B Mater Biol Med. 2016;4(15):2620–7.
148. Guo LX, Hu XL, Guan P, Du CB, Wang D, Song DM, et al. Facile preparation of superparamagnetic surface-imprinted microspheres using amino acid as template for specific capture of thymopentin. Appl Surf Sci. 2015;357:1490–8.
149. Xu XQ, Deng CH, Gao MX, Yu WJ, Yang PY, Zhang XM. Synthesis of magnetic microspheres with immobilized metal ions for enrichment and direct determination of phosphopeptides by matrix-assisted laser desorption ionization mass spectrometry. Adv Mater. 2006;18(24):3289–93.
150. Liu YB, Wang SS, Zhang C, Su X, Huang S, Zhao MP. Enhancing the selectivity of enzyme detection by using tailor-made nanoparticles. Anal Chem. 2013;85(10):4853–7.
151. Wan W, Han Q, Zhang XQ, Xie YM, Sun JP, Ding MY. Selective enrichment of proteins for MALDI-TOF MS analysis based on molecular imprinting. Chem Commun. 2015;51(17):3541–4.
152. Qin YP, Li DY, He XW, Li WY, Zhang YK. Preparation of high-efficiency cytochrome c-imprinted polymer on the surface of magnetic carbon nanotubes by epitope approach via metal chelation and six-membered ring. ACS Appl Mater Interfaces. 2016;8(16): 10155–63.

153. Duan HM, Wang XJ, Wang YH, Sun YL, Li JB, Luo CN. An ultrasensitive lysozyme chemiluminescence biosensor based on surface molecular imprinting using ionic liquid modified magnetic graphene oxide/β-cyclodextrin as supporting material. Anal Chim Acta. 2016;918:89–96.
154. Tan L, Yu Z, Zhou X, Xing D, Luo X, Peng R, et al. Antibody-free ultra-high performance liquid chromatography/tandem mass spectrometry measurement of angiotensin I and II using magnetic epitope-imprinted polymers. J Chromatogr A. 2015;1411:69–76.
155. Madrakian T, Afkhami A, Mahmood-Kashani H, Ahmadi M. Superparamagnetic surface molecularly imprinted nanoparticles for sensitive solid-phase extraction of tramadol from urine samples. Talanta. 2013;105:255–61.
156. Kolaei M, Dashtian K, Rafiee Z, Ghaedi M. Ultrasonic-assisted magnetic solid phase extraction of morphine in urine samples by new imprinted polymer-supported on MWCNT-Fe_3O_4-NPs: central composite design optimization. Ultrason Sonochem. 2016;33:240–8.
157. Yang ZY, Cai QZ, Chen N, Zhou XM, Hong JL. Selective separation and identification of metabolite groups of Polygonum cuspidatum extract in rat plasma using dispersion solid-phase extraction by magnetic molecularly imprinted polymers coupled with LC/Q-TOF-MS. RSC Adv. 2016;6(15):12193–204.
158. Svetushkina E, Puretskiy N, Ionov L, Stamm M, Synytska A. A comparative study on switchable adhesion between thermoresponsive polymer brushes on flat and rough surfaces. Soft Matter. 2011;7:5691–6.
159. Wu Q, Wu DP, Guan YF. In vivo fast equilibrium microextraction by stable and biocompatible nanofiber membrane sandwiched in microfluidic device. Anal Chem. 2013;85(23):11524–31.
160. Zhu CH, Lu Y, Chen JF, Yu SH. Photothermal poly(N-isopropylacrylamide)/Fe_3O_4 nanocomposite hydrogel as a movable position heating source under remote control. Small. 2014;10(14):2796–800.
161. Han H, Lee JY, Lu XM. Thermoresponsive nanoparticles + plasmonic nanoparticles = photoresponsive heterodimers: Facile synthesis and sunlight-induced reversible clustering. Chem Commun. 2013;49(55):6122–4.